REVIEWER 1:

This manuscript examines pulses of NH3 observed by the IASI-A instrument on MetOp- A over the Sahel. These pulses occur at the start of the rainy season and appear to correspond to increased biochemical activity in soils induced by rainfall. The paper is well written, the analysis is clear, and the results are very interesting. My main concern is that the timing of the enhancements in OMI NO2 (May-June), IASI NH3 (March-April), and surface NH3 (May-June) appear to be different. I elaborate on this below.

The timing of the NH3 peaks seems to be different than those of NO2. Several studies (for example Jaeglé et al., 2004; Hudman et al., 2012) have examined satellite NO2 pulses over the Sahel, finding that the pulses take place sometime in May-June, corre- sponding to the arrival of the first rains after the dry season over various regions of the Sahel. Figure 2, shows the same pattern of the largest OMI NO2 enhancement taking place in June. For NH3, the authors focus mostly on March and April. Some discus- sion of why the timing would be different in terms of pulses of NO2 and NH3 would be useful to include in the manuscript (for example in section 3.2.3 discussing the co-emissions of NH3 and NO2). Does it have to do with different population dynamics of the various bacteria and their response to subsequent wetting events? Interestingly, Figure 3 shows that surface observations do indicate maximum NH3 mixing ratios in May-June (at least for sites b, c, f), consistent with the OMI NO2 pulses. Why would surface observations of NH3 show a different seasonality than the satellite observa- tions of NH3? Is the increasing cloud cover affecting the number and quality of the retrievals in May-June? Is the later June NH3 pulse masked by clouds?

This is an excellent question, and we are happy to add more discussion regarding what is happening. In the following, we've broken our response into sections for each major question, and then present the new discussion added to the revised manuscript.

1) Why do we see NH3 pulses in March and April when Jaegle et al 2004 and Hudman et al 2012 find that "pulses take place sometime in May-June, corresponding to the arrival of the first rains after the dry season over various regions of the Sahel?" Our first point is that we believe we have presented evidence that soil NO pulses are occurring in response to the same increases in soil moisture that cause the soil NH3 pulses in March and April 2008, and it seems to us that similar pulsing is observed in both the Jaegle et al 2004 and Hudman et al 2012 papers. As noted on page 14 line 11, satellite observations of NO2 and NH3 concentrations are strongly correlated for the month of April 2008 (r=0.78, p<0.0001), suggesting that the increases in soil moisture are leading to pulsed emissions of both gases. The following figure may help to illustrate the correlation; it reproduces the data included in the top and bottom panels of figure 2 in a single panel (note that each date's means are calculated using only grid cells for which both NO2 and NH3 observations were present):

NH3 vs. NO2, 5-day running mean 2008
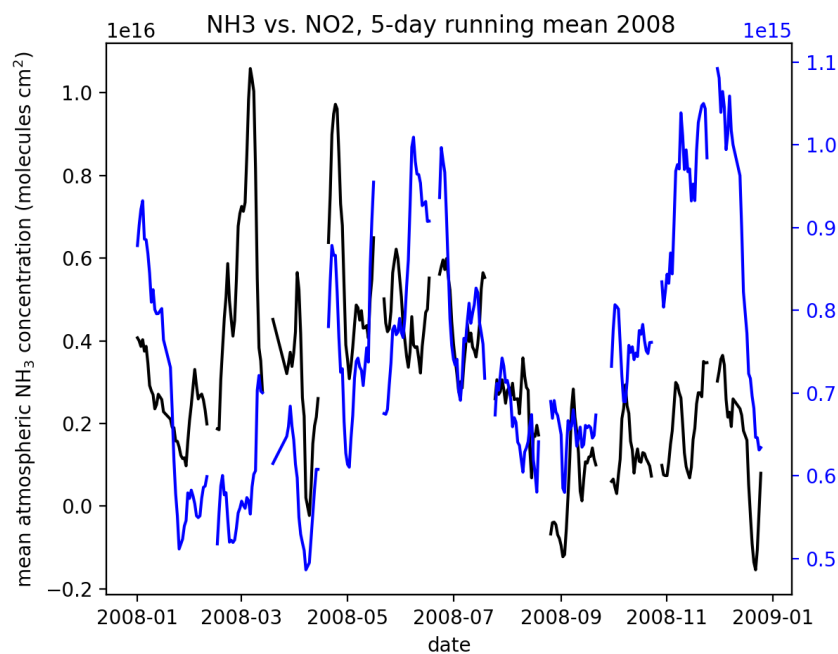
The correspondence of the NO2 and NH3 peaks in April is fairly clear here. We also interpret the March NH3 peak to be accompanied by an NO2 peak that emerges about a week later. We discuss the apparent lag between emission pulses of NH3 and NO2 in March on page 14, line 24 and following, and expand upon it in the revised manuscript (details below). The general idea is that populations of nitrifying bacteria, which are generally responsible for the vast majority of NO emissions from soils, are likely dormant when this March increase in soil moisture occurs. Nitrifiers are notoriously slow growing, resulting in the lag between the pulse of NH3 and NO (in California field soils, no increase in nitrifying populations was observed for the first seven days following fertilizer applications (Okano et al 2004 Appl Env Microbiol.); nutrient additions are physically quite different from wetting, but both do represent release from an environmental limitation on growth). Lags are often observed between wetting or fertilization of soils and subsequent NO emissions from soils in experimental studies. This increase in soil moisture in March is also very modest, which may have limited the magnitude of the NO response more than that of the NH3 response—that is, the increase in soil moisture may have been large enough to trigger a flush of N mineralization and more-or-less immediate NH3 volatilization, but the soils may have dried again before the nitrifying populations were able to really kick into gear (or grow in size), limiting the magnitude of the NO pulse.

Something else to note is that Hudman et al.'s (2012) analysis of atmospheric NO2 concentrations in 2006 uses a 2mm rainfall threshold to define the start of the rainy season. That threshold that is indeed met for much of the Sahel in April of that year, as illustrated in their Figure 2, and thus the pulsing that Hudman et al observe includes pulsing in April. Those patterns are arguably broadly consistent with what we observe here, and the increase in soil moisture we observe in March occurs with average rainfall well under 2 mm (figure 2). The NO2 enhancements that Hudman et al observe are increases roughly between 1 and 1.5 times higher than concentrations 5 days previous to the first rainfall event for a given pixel, which are similar to the enhancements in NO2 we observe during both the March and the April pulse events. (We recognize that Hudman et al do not identify a lagged response, though again, that lag occurred in March, in response to average rainfall below 2 mm.) Jaegle et al focus on enhancements in June, but if you look at the annual data presented in their figure 2, the overall pattern is quite similar to what we observe in 2008: two early modest rainfall events in April and May appear to be accompanied by pulses in NO2 concentration.

2) If it is agreed that there is, in fact, pulsing of both NO2 and NH3 in response to the same increases in soil moisture in March and April, then the question becomes "why do NO2 concentrations reach their maxima in May and June, whereas the NH3 concentrations reach maxima in March and April?" This again is a good question. We believe it is probably related to the different mechanisms responsible for emissions of NH3 and NO from soils, and potentially in part to the dependence of both processes on ammonium (NH_4^+) availability. NO is primarily produced biologically during two processes: the transformation of NH4+ to nitrate during nitrification, and the transformation of nitrate to N2 during denitrification. NH3 is produced abiotically when ammonium is deprotonated. We mentioned above the slow-growth of nitrifying populations; generation times of 373 hours were observed for population responses of ammonia oxidizers to ammonium sulfate applications in a maize field in Davis, California (Okano et al 2004 Appl Env Microbiol.). In that example, population size did not increase at all during the first week following the ammonium sulfate applications, and rose by roughly 50% during the second week. Between the 13th and 39th day, however, the population roughly tripled. This is just one study, and it is looking at the effects of fertilizer application rather than of wetting (although it was conducted in the early growing season in a region with distinct rainy and dry seasons, and both wetting and fertilization represent a release from environmental constraints on population growth), but the slow rate of nitrifying population growth observed in Davis matches the patterns observed over the Sahel very well: nitrifying populations are presumably released from widespread water limitation starting around the end of April, and NO concentrations grow to their maximum a little more than a month later.

A second point here is that both NH3 volatilization and nitrification are dependent on the availability of NH4+, and thus we can potentially explain why NH3 concentrations decline somewhat when NO2 concentrations increase: growing nitrifying populations represent more competition for available NH4+. Some researchers have suggested that this competition is so steep that the two processes are mutually exclusive (Praveen-Kumar and Aggarwal, 1998). As environmental conditions become more

accommodating for nitrifying populations, NH3 emissions could be expected to necessarily decrease as NO emissions increase, all else being equal. However, it is interesting to note that at 167 mg N m^{-2}, the mean total NH3 emissions per unit area for the 61-day period in May and June are still quite elevated relative to the dry season, just a slight decline from the 61-day period in March and April (173 mg N m^{-2}). So it would appear that both periods are important for NH3 emissions, although in March and April, the pulsing dynamics appear to be much more distinct and important.

3. Could changing NH3 observation counts be responsible for the mismatch? It does not appear so. Although there is a drop in observation counts in July and August, for the period of March through the end of June (green points in the plot below), observation counts are relatively constant. In addition, in our original correlation analysis, we only used grid cells that included both NO2 and NH3 observations; in our presentations in figures 2 and 6, we included NO2 grid cells that also had NH3 observations, and so any change in NH3 observation counts would have affected the temporal patterns of both gases equally. In this revision, we include additional analyses that consider only grid cells where both NH3 and NO2 observations, with no qualitative effect on the results (see response to Reviewer 2's comment regarding Page 18, line 10 below).
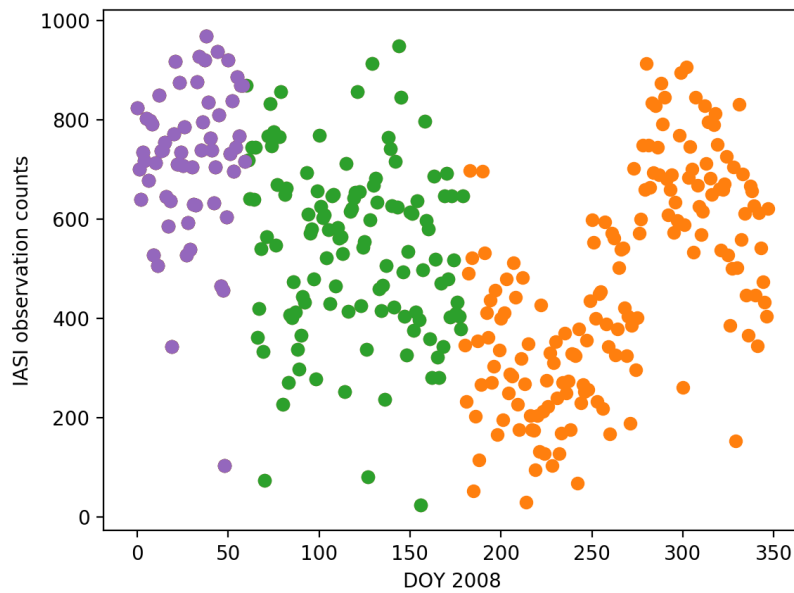
4. Why is there an apparent mismatch between INDAAF surface observation sites and satellite observations of NH3? Another good question. Spatial variation in the timing and magnitude of NH3 emissions and concentrations is to be expected, and we believe that the basic issue is that these sites are not representative of the mean for our focal region of the Sahel. When examining patterns of monthly mean NH3 concentrations for 1° grid cells centered on each of the three INDAAF Sahel sites (b, c, and f), we see that the overall pattern for 2008 observed by IASI and at the surface is in better agreement with the surface observations than the regional mean of IASI observations is.
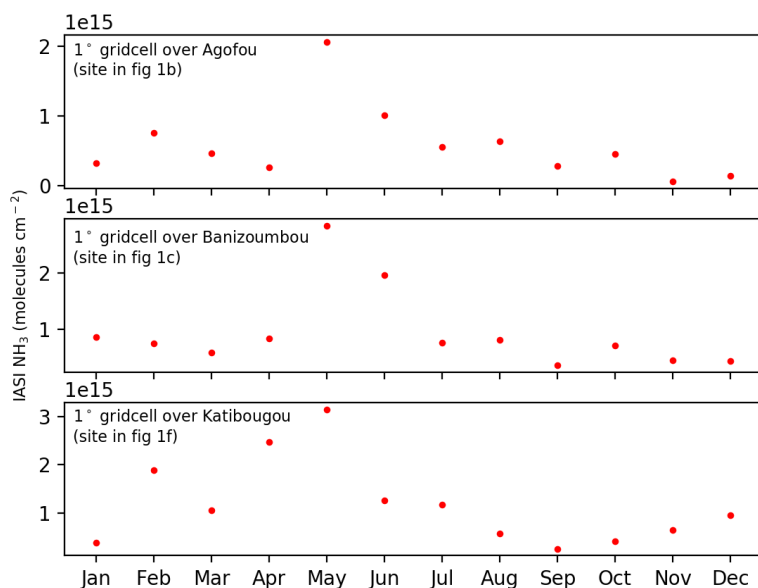
In these satellite observations of the atmosphere over each of the surface sites, the increase in spring NH3 concentrations occurs later in the year than the regional mean, with peak NH3 concentrations occur in May for each location. This is perhaps not surprising, since our focal region is characterized by a gradient of increasing mean annual precipitation from north to south, combined with generally earlier onset of the rainy season in the south than the north. Hence, we may expect to see earlier and/or larger NH3 emissions from the southern than the northern part of the region on average (e.g., Figure 5 in the original manuscript), and the INDAAF Sahel sites are largely in the northern part of the latitudinal range we examine.

Praveen-Kumar and Aggarwal, R. K.: Interdependence of ammonia volatilization and nitrification in arid soils, Nutr. Cy. Agroecosys., 51, 201–207, doi:10.1023/A:1009720003490, 1998.

NEW DISCUSSION TEXT:

Page 15, line 20 and following: "There is also a clear mis-match in the timing of the peak NH3 concentrations, which occurred in March and April, and peak NO_2 concentrations, which occurred in May and June (Figure 2). We believe that several factors are likely contributing to the different temporal dynamics of NH3 and NO2 concentrations. First, to be clear, we argue that the rainfall events in March and April are indeed triggering pulses of both gases, illustrated in part by the strong correlation between the two gases during April (r=0.78, p<0.0001; Figure 2; for a strict comparison in which concentrations of NO2 and NH3 are calculated using only grid cells that have observations for both gases, see Figure S1, though the results are qualitatively similar to Figure 2). Temporal patterns of surface NO_2 concentrations observed by the INDAAF network may also support the presence of these smaller, early pulses (Figure S2). Although not explicitly investigated, we believe earlier studies of NO2 pulsing in the Sahel that focus on emissions during May and June include observations of similar early season pulses (Jaegle et al. 2004, Hudman et al. 2012).

The smaller early season NO2 pulses are potentially the result of the nitrifier population dynamics alluded to above. Specifically, because population growth is slow, nitrifying populations are smaller during March and April than they will become later in the growing season when they are released from sustained environmental limitations on growth, and so nitrification rates remain lower in these early responses. In an earlier field study conducted in Davis, California, which also experiences distinct dry and rainy seasons, nitrifier population growth rates were very slow to respond to ammonium additions, roughly matching the temporal patterns of NO2 emissions we observed in the Sahel (Okano et al. 2004). In that study, population size did not increase during the first week following ammonium sulfate applications, and then rose by roughly 50% in the second week. Between the 13th and 39th day, however, the population roughly tripled. In the Sahel, nitrifying populations are presumably released from widespread water limitation around the beginning of May (Figure 2), and NO2 concentrations grow to their maximum a little more than a month later. An additional point is that although the pulsing behaviour of NH_3 appears to diminish in May and June, total NH_3 emissions during those months are almost as elevated relative to the dry period as emissions during March and April (167 mg N m^{-2} and 173 mg N m^{-2} for each 61-day period, respectively; Figure 6). Consequently, it could be argued that May and June remain important months for both NO_2 and NH_3 emissions. For a presentation of modelled emissions calculated based only grid cells that have satellite observations for both gases, see Figure S3. This additional screening reduces annual modelled NH_3 emissions by roughly 5%, and reduces modelled emissions during the pulses by roughly 2-3% relative to modelled NH_3 emissions that do not take the presence or absence of NO_2 observations into account.

A second point is that both NH_3 volatilization and nitrification are dependent on NH_4^+ availability, and thus competition between these processes for NH_4^+ is likely to contribute to the observed temporal dynamics of atmospheric NH_3 and NO_2 concentrations. The increased competition for available NH_4^+ from growing nitrifier

populations could contribute to the observed decline in NH_3 emissions between April and May. Earlier researchers have hypothesized that competition between NH_3 volatilization and nitrification for NH_4^+ is so extreme that the two processes cannot occur at the same time (Praveen-Kumar and Aggarwal, 1998). However, soil emissions of NO and NH_3 have been shown to be broadly coupled in the Sahel (Delon *et al.* 2018), and the few field and lab studies measuring soil emissions of both gases following wetting observe positive fluxes of each (McCalley and Sparks, 2008; Schlesinger and Peterjohn, 1991; Soper et al., 2016), with NH_3 dominating emissions from desert soils (McCalley and Sparks, 2008; Schlesinger and Peterjohn, 1991) and NO dominating from grassland soils (Soper et al., 2016). Our findings contrast with those of Soper et al., as NH_3 appears to be the dominant species emitted during pulse events in March and April (Figure 6), though NO may dominate later in the season, during the period focused on by Jaeglé et al (2004). We expect that even were the two processes mutually exclusive at the scale of a soil core or chamber, heterogeneity in soil properties at the pixel or regional scale would explain our observations of coinciding peaks of NO_2 and NH_3."

Page 19, line 15 and following: "The difference in the timing of peak NH_3 concentrations between the IASI observations and surface observations at Banizoumbou and Katibougou may be in part because of random variation and the effects of local influences, which are likely also responsible for variation among the three sites. In addition, deterministic variation in NH_3 emissions in the Sahel is likely important. These sites are located at latitudes near the northern boundary of our focal area, and could be influenced by emissions from the north. In addition, we observe a north-south gradient in soil moisture, precipitation, and NH_3 concentrations during the pulse event in April (Figure 4), suggesting that pulsing is larger in the southern part of our focal area during this period. The onset of the rainy season tends to occur later in more northern latitudes. Indeed, IASI observations of 1° gridcells over each of the three INDAAF sites show better agreement with the surface observations, with peak NH3 concentrations occurring in May for all sites during 2008 (Figure S4)."

Minor comments. - Throughout the manuscript (including the abstract). The authors refer to NO2 as 'nitric dioxide'. It should be nitrogen dioxide.

Thank you for catching this error, though we want to point out that it occurred only once (in the abstract: page 1, line 20). Throughout the manuscript, we use nitric oxide (NO) when discussing soil emissions, and nitrogen dioxide (NO2) when discussing OMI observations. We recognize that this could lead to some confusion, but also believe it is a precise description of the processes and observations discussed in the manuscript (suggestions for improving clarity are welcome). We have made a few changes for improved accuracy and to try to minimize any confusion. We also include the following statement to highlight our use of NO, NO2, and NOx in the manuscript:

"Note that in this paper, NO is used in discussions of soil emissions specifically; since satellite observations are of NO_2, we use NO_2 when discussing those observations, and NO_2 or NO_x when discussing modelled surface emissions based on those observations." (Page 5, line 17)

Some example changes; in these examples, "NO2" was formerly "NO" and "peak" was formerly "pulse" (new text in bold italics):

"The March *NO₂ peak* is also smaller than the April *NO₂ peak*, and smaller than the April NH₃ *peak*."

"We expect that even were the two processes mutually exclusive at the scale of a soil core or chamber, heterogeneity in soil properties at the pixel or regional scale can explain our observations of coinciding *peaks* of *NO₂* and NH₃."

"In general, however, our modelled emissions suggest that NH₃ is probably emitted at substantially higher rates than NO *or NO₂* during pulse events,"

"limit our ability to quantitatively constrain the surface NH₃ or **NO₂** fluxes, or to make strict quantitative comparisons between them."

- Equation 1. It isn't clear how this is used for low concentrations. Does the equation mean that even if the error is above 100%, if the concentrations are low enough then the retrievals are kept? Also, it would be useful to have units after 5x1015 (I assume it is molec/cm2)

It does indeed mean that if the concentrations are low enough then the retrievals are kept. The errors are based on a statistical analysis of variability in the retrieval parameters observed over a clean patch in the pacific (Whitburn 2016). But under the right conditions, it is possible that a retrieval is correct while the error (being slightly fixed) is too high, and so the equation allows for retaining these low concentration retrievals. This also resolves the issue of biasing high when removing all small values (as most have a relative error above 100). And thank you: we have added the units to the equation.

Whitburn, S., Van Damme, M. and Clarisse, L.: A flexible and robust neural network IASI-NH3 retrieval algorithm, J. Geophys. Res.-Atmos., 121, 6581–6599, doi:10.1002/(ISSN)2169-8996, 2016

- Equation 3. There is an extra space before the tx (effective lifetime), also, x should be subscripted.

We have made the changes

REVIEWER 2:

8

I have read the comments from the first reviewer and agree that this is a clear, well written and very interesting paper. I also agree that the offset between the NH3 and NO2 peaks should be discussed in slightly more depth. What does the INDAAF NO2 data show?

INDAAF NO2 observations (as illustrated in the following figure) follow a broadly similar pattern to the OMI NO2 observations, with the highest concentrations occurring in May and June in Banizoumbou (c), Katibougou (f), and possibly in Agoufou (b), though data for June 2008 are not available. The pattern in Agoufou and Banizoumbou are interesting, with elevated concentrations in April (and March for Banizoumbou) in 2008, but with peak NO2 concentrations occurring in May and June (Banizoumbou) or June and July (Agoufou long-term average). These data suggest the presence of smaller early season NO pulses in these sites. Katibougou is also very interesting: the concentration peak occurs in May, with a substantial decline in June. We include the following figure as SI for the revised manuscript.
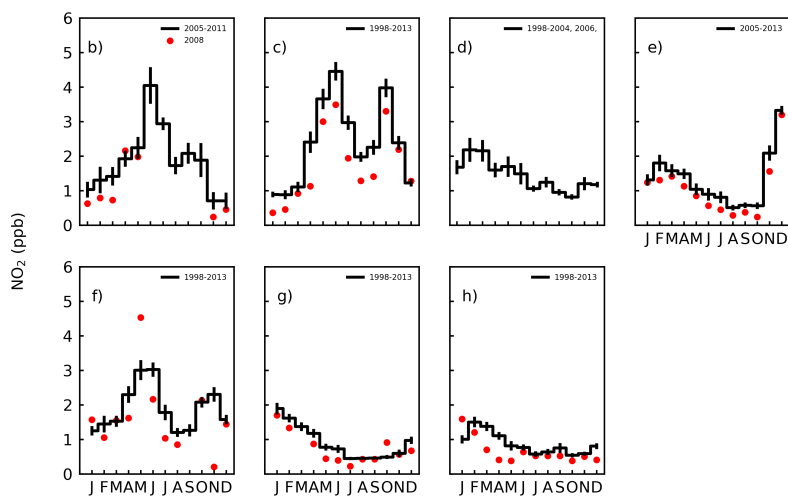
Agoufou, Mali (b), Banizoumbou, Niger (c), Bomassa, Congo (d), Djougou, Benin (e), Katibougou, Mali (f), Lamto, Côte d'Ivoire (g), and Zoetele, Cameroon (h).

It appears to us that the patterns here reflect both the possibility of early season pulses in Agoufou and Banizoumbou, and also the presence of substantial variability in the timing of peak concentrations among the three sites located within the Sahel. That spatio-temporal variability in the timing of peak NO2 concentrations would seem to highlight the potential importance of local influences which can contribute to different patterns between sites, and potentially between surface and satellite observations.

I do think some clarification from the authors would be helpful on the following issues:

Page 7, line 7: please add a sentence of two on the regridding technique used.
   We have added the additional clarifying sentence (Page 7, line 14): "*Specifically, we calculated the concentration for a given grid cell as the mean of all elliptical IASI footprints for which the corners of the grid cell were within the footprint.*"
Page 7, line 11: what is the IASI detection limit in the Sahel?

This is a difficult question to answer as there aren't any hourly measurements available in the Sahel region, which makes it hard to compare the conditions with the satellite observations. However, the Sahel is a region with high thermal contrast (in contrast to, say, northern Europe), which makes it a region with generally optimal conditions for IASI. From comparisons with measurements under conditions of high thermal contrast, IASI seems to be able to reliably observe down to 1 to 2 ppb at the surface, which translates roughly into ~2e15/5e15 depending on the boundary layer height and other factors. This level of sensitivity is also seen in Van Damme et al., 2015 and Dammers et al., 2016, which found acceptable correlations between IASI and independent observations, even for background-like concentrations. We have added the following text (page 7 line 9):

"Given the absence of hourly observations in the Sahel, the detection limit of IASI is difficult to determine with certainty. However, the region experiences high thermal contrast, and IASI seems to be able to reliably observe down to 1 to 2 ppb at the surface."

Page 8, line 24: it appears that a uniform profile is assumed here. Is this really a good assumption?

Good point, and one we should have highlighted in the original manuscript. This is a simplifying assumption, which we have made for three key reasons: 1) We believe that given the level of uncertainty inherent in our box model (with its assumptions of no transport and the use of a range of plausible effective lifetimes of NO2 and NH3), it is preferable to keep the model as simple as possible to both make it as transparent as possible, and to avoid giving the impression of a level of accuracy or certainty in modeled emissions that is not present, especially given the uncertainty in vertical distribution of NH3 in the IASI retrievals. 2) Independent of point 1, we do not think the assumption is unreasonable. The vertical profile of IASI NH3 is assumed to be essentially homogeneous within the boundary layer. And since lifetimes of both gases are relatively short, it seems plausible that gases are concentrated near the surface, especially when concentrations are most influenced by soil fluxes. 3) Lastly, we decided to take an identical modeling approach to that of Whitburn et al 2015 in modeling NH3 fluxes so that the results of the

two studies, which focus on adjoining regions in Africa and contrasting sources of NH3, are strictly comparable.

In addition to emphasizing the simple nature of the box model in the text, we have added the following clarifying text (Page 17, line 26):

"It is also important to note the simplifying assumption of a uniform atmospheric profile in the box model, which ignores any variation in vertical distribution. Still, we believe a uniform profile is a reasonable assumption, especially for soil fluxes. Each of these gases has relatively short lifetimes, and unlike fire plumes, are unlikely to be rapidly lofted to high altitudes following emission from soil. In addition, there is very little variation in NH3 distribution throughout the boundary layer in the assumed IASI profile."

Whitburn et al. 2015 Atmos. Env. 121: 42e54

Page 11, line 11: I don't see the increase in fire emissions in late March

Thank you for pointing out this error; the modest increase is actually just prior to the April pulse, not the March pulse. We have revised the paragraph to read as follows (Page 11, line 16; changes in bold italics):

"For our focal region of the Sahel (defined above and outlined in red in Figure 1), mean atmospheric NH_3 concentrations exhibit two distinct peaks in late March and April (Figure 2a, highlighted in light and dark pink, respectively), which represent the highest concentrations observed in 2008. ***The late March peak occurs at the same time as an apparent modest increase in mean soil moisture (Fig 2b).*** The peak in April, during which atmospheric NH_3 concentrations over the Sahel are elevated relative to other parts of north equatorial Africa (Figure 3a), occurs during the first period of sustained rainfall in the focal region, and corresponds to a peak in soil moisture, suggesting a possible causal relationship between changes in soil moisture and atmospheric NH_3 concentrations (Figure 2b and section 3.2.1 below). ***This April peak does occur following a possible modest increase mean fire emissions (Fig 2a) across the Sahel***. Overall, however, the seasonality in IASI-retrieved atmospheric NH_3 concentrations exhibits a marked difference from the seasonality in GFED4s NH_3 emissions from fires, which start increasing in September and peak in November (Fig 2a and section 3.2.2 below). "

Page 12, line 25: It could be helpful to rewrite this as: " except during the biomass burning season"

We have revised the sentence to read as follows (Page 13, line 8; added text in bold italics):

"A comparison between our simple box model estimates of NH_3 flux and emissions from the GFED4s inventory strongly supports the hypothesis that biomass burning does not play an important role in NH_3 emissions during March or April, and further suggests that biomass

burning may represent a relatively unimportant regional source of NH₃ during most of the year, ***outside of the biomass burning*** *season* (Figure 6)."

Page 13, line 23: at what scale where these correlations calculated: 0.25 deg or over the entire box?

 The correlations were calculated over the entire box; we have revised the sentence to clarify (Page 14, line 10; new text in bold italics):

"For the month of April, total column NH₃ concentrations and tropospheric NO₂ concentrations ***integrated across the entire focal region*** are strongly correlated (r=0.78, p<0.0001)."

Page 15, line 22: possibly repeat that IASI NH3 appears to be biased low

Thank you for the suggestion. We have revised the paragraph to read as follows (Page 17, line 16; new text in bold italics):

"During the early growing season, atmospheric concentrations of NH₃ are roughly an order of magnitude higher than NO₂ (figure 2). It is important to note that NH₃ retrievals generally have a higher error, and that our screening process may introduce a potential bias in that we permit retrievals with higher uncertainty if they are low concentrations; we also retain observations of negative concentrations. ***In addition, as mentioned earlier, compared to FTIR observations the IASI total columns are biased low by ~30% which varies per region depending on the local concentrations***. From this perspective, our concentration and emission estimates can be considered conservative."

Page 17, line 17: only NO2 concentrations become comparable to NH3, not the fluxes

 Well noted—as it turns out, neither NO2 concentrations nor fluxes are comparable in magnitude to those of NH3 (note the differences in scale in figure 2, something we clearly failed to do adequately), so thanks very much for catching this mis-statement. We have revised the sentence to read as follows (Page 20, line 14; new text in bold italics, including new text to clarify the time period being discussed):

"After the early season pulses, NH₃ concentrations and fluxes remain fairly elevated (figure 2, 6); during this period ***of May through July***, NO₂ concentrations and fluxes increase, becoming ***closer*** in magnitude to NH₃ (figure 2,6)."

Page 18, line 8: a more sophisticated inverse modeling of the emissions? This should be made clearer, and should suggest an approach

This point is really just intended to acknowledge that our emissions modeling is extremely simple, and that, for example, inverse modeling using a Kalman filtering or Bayesian approach and an atmospheric chemical transport model could potentially provide more insight into surface

emissions. We add the following text to provide an illustration and example of what is intended with this statement (Page 21, line 4; new text in bold italics):

"A more sophisticated inverse modelling approach *(e.g., using a Bayesian approach in combination with an atmospheric chemical transport model)* could provide firmer insight into the magnitude of emissions, as well as provide some insight into the magnitude of specific NH$_3$ sources."

Page 18, line 10: the increased cloud cover during the rainy season could certainly mask increased NH3. Cloud cover would also impact OMI NO2, but possibly not to the same degree. If at all possible, the authors should discuss this.

A good point. In the original manuscript, for the correlation analysis between satellite NO2 and NH3 observations, only grid cells including observations of both gases were used in the analysis, and so no effect of cloud cover should be present in that analysis. In contrast, figures 2 and 6 (which present both NO2 and NH3 data), are based on OMI-NO2 observations only from grid cells that also had IASI-NH3 observations. The reasoning for not also screening NH3 observations based on whether NO2 observations were present was that the focus of the manuscript is NH3, and the NO2 data were intended as a complementary measure that could provide insight into the mechanism behind the NH3 pulses. We agree that clearly illustrating and discussing the mismatch between NH3 and NO2 responses to wetting events is important, and so in revision, we include additional analyses restricted to grid cells that have both IASI and OMI observations, resulting in new versions of figures 2 and 6 (included below as Figures S1 and S3, respectively); these figures suggest that the different seasonality of the two gases is not an artifact of different impacts of cloud cover on the two satellite products. We have decided that in the main text of the manuscript it is more appropriate to present NH3 that is not screened based on the presence of NO2 observations, and to include the new versions in the supplemental information: we feel that the goal of presenting as complete a picture of the seasonality of NH3 concentrations as possible takes precedence over the goal of comparing NH3 and NO2 patterns. We do refer to the two new figures at Page 15 line 26 and Page 16 line 20:

> "for a strict comparison in which concentrations of NO2 and NH3 are calculated using only grid cells that have observations for both gases, see Figure S1, though the results are qualitatively similar to Figure 2"

> "for a presentation of modelled emissions calculated based only grid cells that have satellite observations for both gases, see Figure S3. This screening reduces annual modelled NH$_3$ emissions by roughly 5%, and reduces modelled emissions during the pulses by roughly 2-3% relative to modelled NH$_3$ emissions that do not take the presence or absence of NO$_2$ observations into account."

When including only grid cells with both NH3 and NO2 observations, there is little qualitative change in seasonal patterns. In the revised figure 6 (Figure S3), we also use screened GFED NO2 and NH3 data, so that only observations from pixels where the respective satellite observations also exist are included in calculating the daily means presented to allow for a more direct comparison to modelled fluxes; again, there are no qualitative changes in the patterns observed. We also did a small quantitative check on the effect on modelled emissions of screening NH3 based on NO2 observations, and found that doing so results in a decline in total annual modelled emissions of

13

roughly 5%, and a decline in emissions during the pulses of roughly 2 to 3%, making the pulses slightly smaller but slightly more important in the context of annual emissions.

In addition, in re-visiting our screening process, we realized that we had used the wrong mask to prepare the NO2 data for the box model and figure 6. We have since done a thorough check to ensure that the masks and analyses conducted for the revision were completed as intended. The change in mask does not affect the results qualitatively; there is, however, a substantial increase in the magnitude of modelled NO2 emissions. Only figure 6 is affected by the change (the correct mask was used in preparing figure 2). We have revised figure 6, and deleted the phrase "possibly by a factor of 10 or more," originally on page 15 line 27.
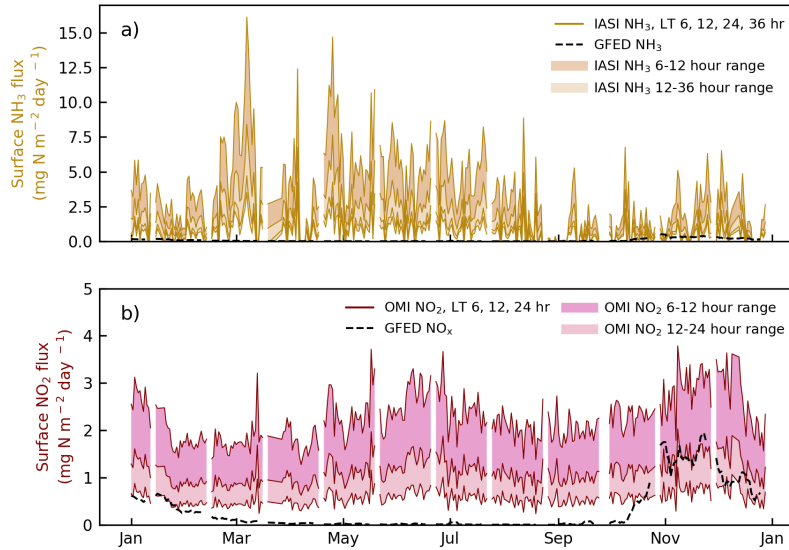

Figure S3. *Comparison of daily total surface fluxes and biomass burning emissions of a) NH$_3$-N and b) NO$_2$-N for the focal study region in the Sahel during 2008.* Total surface fluxes are estimated from IASI NH$_3$ and OMI NO$_2$ observations using a simple box model and assuming effective lifetimes of 12, 24, or 36 hours for NH$_3$ and of 6, 12, or 24 hours for NO$_2$. Fire emissions are taken from the GFED4s database. Modelled and GFED4s mean emissions were calculated using values only of 0.25° grid cells within the study region for which both NO$_2$ and NH$_3$ observations were present. Note the difference in scales, and that shorter effective lifetimes result in higher modelled emissions.
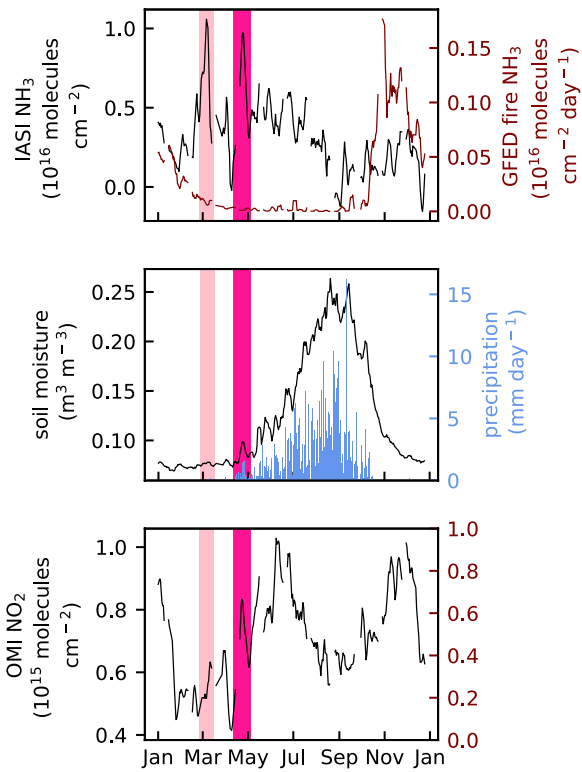
14

Figure S1: *Early growing season NH₃ pulses temporally associated with changes in soil moisture and with NO₂ pulses over the focal study region in the Sahel during 2008.* Top panel: Daily atmospheric NH₃ concentrations from IASI and NH₃ biomass burning emissions from GFED4s. Middle panel: ESA-CCI soil moisture and TRMM precipitation. Bottom panel: atmospheric NO₂ concentrations from OMI. Putative soil emission pulses in March and April are highlighted in bright and dark pink, respectively. The means of all variables presented were calculated using values of 0.25° grid cells within the study region for which both NO₂ and NH₃ observations were present. GFED4s emissions were converted from a mass-based to molecule-based flux to allow comparison with the IASI retrievals; note the different scales for the left and right y axes of the top panel.

15

Minor comments:

Page 4, line 27: the second sentence does not follow from the first

We presume the issue being raised here is the use of the East African example and the leap from a discussion of environmental conditions to examples of ammonia emissions being structurally inelegant (a point we agree with). We have re-written the paragraph as follows (page 4 line 15; moved or added text in bold italics):

"Given the importance of rainfall seasonality, soil pH, and N availability in contributing to NH_3 emission pulses, soils in the Sahel may be an important source of NH_3 to the atmosphere during the onset of the rainy season*, and a case study for determining whether Birch effect NH_3 pulsing is an important process at broad regional scales*. The Sahel is a grassland environment representing a transition between desert and productive savannas. It is characterized by a unimodal rainfall seasonality, with mean annual precipitation typically ranging between 100 and 600 mm yr^{-1}. Seasonal variation in rainfall is broadly determined by movement of the Intertropical Convergence Zone (ITCZ). Migration of the ITCZ north of the equator in the first half of the calendar year is accompanied by the onset of the rainy season and West African Monsoon, with the first substantial rain events occurring in April. The southward retreat of the ITCZ marks the dry season *in the Sahel* starting in October or November. Recent maps of African soils based on surface reflectance suggest that soils across the Sahel tend to have pHs largely near neutral, but can be higher than 9 in some areas (Vågen et al., 2016). The combination of seasonal rainfall variability and soils with neutral or alkaline pHs suggests that Sahelian soils may be an important source of NH_3 at the onset of the rainy season. Although the Sahel has regions of relatively dense cropland, it is characterized by lower levels of fertilizer inputs (FAO, accessed 2018) and smaller loads of atmospheric N deposition (Dentener et al., 2006; Galy-Lacaux and Delon, 2014; Laouali et al., 2012; though deposition can be elevated at the Sahel's southern boundary) than other parts of the world. However, it has moderately high livestock densities (Robinson et al., 2014), potentially providing sites of abundant available N for the production of NH_3. *Indeed, soil NH_3 emissions have been shown to be higher at a site in northern Senegal following a rain event (Delon et al., 2017).*"

Page 7, line 7: IASI data are only used if the pixels are 75% cloud-free, while OMI data is included only if the cloud-cover is less than 30%. While these statements are almost equivalent, it would be clearer to say 75% cloud-free and 70% cloud-free, or cloud cover less than 25% and cloud cover less than 30%.

We have changed the description of the OMI level 3 NO2 product as follows (page 8 line 10):

"The product is cloud-screened, including only pixels that are at least 70% cloud-free"

16

Page 9, line 25: "burned area and fuel consumption in savannas are"

Fixed, thank you.

Satellite evidence of substantial rain-induced soil emissions of ammonia across the Sahel

Jonathan E. Hickman[1, *], Enrico Dammers[2], Corinne Galy-Lacaux[3], Guido R. van der Werf[1]

[1]Earth and Climate Cluster, Vrije Universiteit, Amsterdam, 1081 HV, Netherlands
[2]Environment and Climate Change Canada, Toronto, Ontario, M3H 5T4, Canada
[3]Laboratoire d'Aérologie UPS-CNRS UMR 5560, Toulouse, 31400, France
*now at NASA Goddard Institute for Space Studies, New York, NY, 10025, USA

Correspondence to: Jonathan E. Hickman (jonathan.e.hickman@nasa.gov)

Abstract. Atmospheric ammonia (NH_3) is a precursor to fine particulate matter formation and contributes to nitrogen deposition, with potential implications for the health of humans and ecosystems. Agricultural soils and animal excreta are the primary source of atmospheric NH_3, but natural soils can also be an important emitter. In regions with distinct dry and wet seasons such as the Sahel, the start of the rainy season triggers a pulse of biogeochemical activity in surface soils known as the Birch effect, which is often accompanied by emissions of microbially-produced gases such as carbon dioxide and nitric oxide. Field and lab studies have sometimes, but not always, observed pulses of NH_3 after the wetting of dry soils; however, the potential regional importance of these emissions remains poorly constrained. Here we use satellite retrievals of atmospheric NH_3 using the Infrared Atmospheric Sounding Interferometer (IASI) regridded at 0.25° resolution, in combination with satellite-based observations of precipitation, surface soil moisture, and nitrogen dioxide concentrations, to present evidence of substantial precipitation-induced pulses of NH_3 across the Sahel at the onset of the rainy season in 2008. The highest concentrations of NH_3 occur in pulses during March and April, when biomass burning NH_3 emissions estimated for the region by the Global Fire Emissions Database are low. For the region of the Sahel spanning 10° to 16° N and 0° to 30° E, changes in NH_3 concentrations are weakly but significantly correlated with changes in soil moisture during the period from mid-March through April, when the peak NH_3 concentrations occur (r=0.28, p=0.02). The correlation is also present when evaluated on an

Deleted: nitric

1

individual pixel-basis during April (r=0.16, p<0.001). Using a simple box model, average emissions for the entire Sahel are between 2 and 6 mg NH_3 m^{-2} day^{-1} during peaks of the observed pulses, depending on the assumed effective lifetime. These early season pulses are consistent with surface observations of monthly deposition, which show an uptick in NH_3 deposition at the start of the rainy season for sites in the Sahel. The NH_3 concentrations in April are also correlated with increasing tropospheric NO_2 concentrations observed by the Ozone Monitoring Instrument (r=0.78, p<0.0001), which have previously been attributed to the Birch effect. Box model results suggest that pulses occurring over a 35-day period in March and April are responsible for roughly one fifth of annual NH_3 emissions from the Sahel. We conclude that precipitation early in the rainy season is responsible for substantial NH_3 emissions in the Sahel, likely representing the largest instantaneous fluxes of nitrogen gas from the region during the year.

1. Introduction

Ammonia (NH_3) plays an important role in the atmosphere and in the nitrogen (N) cycle. In the atmosphere, NH_3 is a precursor to the formation of fine particular matter ($PM_{2.5}$), which contributes to substantial levels of premature mortality (Lelieveld *et al*., 2015). NH_3 can also form a substantial proportion of atmospheric N deposition (Dentener *et al*., 2006; Holland *et al*., 2005), affecting downwind ecosystems by potentially altering productivity (Thomas *et al*., 2009), soil pH (Tian and Niu, 2015), eutrophication status (Bergstrom and Jannson, 2006), biodiversity (Bobbink *et al*., 2010), and stimulating emissions of other trace gases such as nitric oxide (NO) and nitrous oxide (N_2O; e.g., Eickenscheidt *et al*., 2011; Pilegaard *et al*., 2006).

Cropland and grazed soils have long been known to be a major source of atmospheric ammonia through the volatilization of urea and ammonium (NH_4^+) based inorganic fertilizers as well as of livestock excreta (Bouwman *et al*., 1997). Ammonia emissions can also represent an important N flux in natural ecosystems, particularly in drylands. In deserts, soil NH_3 emissions can represent over 25% of annual nitrogen losses (McCalley and Sparks, 2008) and over 10% in a semiarid savanna (Fiona M Soper, 2016).

Soil moisture is a key control over biogeochemical cycles in drylands (Austin *et al.*, 2004). Biogeochemical cycling in dryland soils is often characterized by pulsing dynamics related to the wetting or re-wetting of dry soils, known as the Birch effect (Birch, 1960; Birch and Friend, 1956). In environments where the distribution of annual precipitation is distinctly seasonal, soil microbial activity typically declines during the dry season, as water becomes limiting and microbes senesce or become dormant (Borken and Matzner, 2009). N may build up in soils during this period, when little biological uptake occurs, but when atmospheric N deposition continues and senesced microbial and plant material accumulates (Borken and Matzner, 2009). The onset of the rainy season can initiate a rapid increase in microbial activity (Birch and Friend, 1956; Borken and Matzner, 2009; Placella and Firestone, 2013; Placella *et al.*, 2012), as re-awakened microbes take advantage of pools of N that accumulated or were made more bioavailable during the dry season, leading to large increases in N mineralization rates (Birch, 1958; 1960; Borken and Matzner, 2009; Dijkstra *et al.*, 2012; Saetre and Stark, 2004; Semb and Robinson, 1969).

The abrupt change in water potential also represents a stress to microbes, prompting a flush of labile N solutes released by microbes to maintain turgor pressure (Kieft *et al.*, 1987). This increase in microbial activity is accompanied by pulsed emissions of trace gases such as carbon dioxide (CO_2; Emmerich, 2003; Huxman *et al.*, 2004; Saetre and Stark, 2004) and NO (e.g., Anderson and Levine, 1986; Davidson, 1992), which can be an important component of annual emissions (Davidson, 1992; Jaeglé *et al.*, 2004). As the availability of NH_4^+ is a major control over NH_3 volatilization (Nelson, 1982; Schlesinger and Peterjohn, 1991), a flush of N mineralization would be expected to trigger an NH_3 emission pulse as well. A few studies have documented pulse dynamics in emissions of NH_3 in laboratory or field settings (Delon *et al.*, 2017; McCalley and Sparks, 2008; Schlesinger and Peterjohn, 1991; Soper *et al.*, 2016). In arid and semi-arid ecosystems, soil NH_3 emissions have been observed to increase by ~15% to 630% after wetting (Schlesinger and Peterjohn, 1991). However, there are few studies outside desert ecosystems (Kim *et al.*, 2012), and an increase in NH_3 emissions following wetting is not always observed (e.g., Yahdjian and Sala, 2010). The potential importance of these pulse emissions of NH_3 at landscape or regional scales remains poorly constrained.

3

In addition to NH_4^+ availability, soil pH is a key environmental control over NH_3 production in soils (Dawson, 1977; Nelson, 1982). Since NH_3 is typically produced through the deprotonation of NH_4^+, NH_3 emissions would be expected to be higher in relatively alkaline soils, or in soil with alkaline microsites. Globally, soils tend to shift from alkaline to acidic when mean annual precipitation exceeds mean annual evapotranspiration (Slessarev *et al*., 2016), so soils in drier biomes such as deserts and grasslands tend to be alkaline (though there are exceptions to this pattern), creating conditions favourable to NH_3 volatilization. For example, the combination of pH and ammonium concentrations in soils from a semi-arid ecosystem in Senegal have been shown to create conditions favorable to the emission of NH_3 (Delon *et al*., 2017).

Given the importance of rainfall seasonality, soil pH, and N availability in contributing to NH_3 emission pulses, soils in the Sahel may be an important source of NH_3 to the atmosphere during the onset of the rainy season, and a case study for determining whether Birch effect NH_3 pulsing is an important process at broad regional scales. The Sahel is a grassland environment representing a transition between desert and productive savannas. It is characterized by a unimodal rainfall seasonality, with mean annual precipitation typically ranging between 100 and 600 mm yr^{-1}. Seasonal variation in rainfall is broadly determined by movement of the Intertropical Convergence Zone (ITCZ). Migration of the ITCZ north of the equator in the first half of the calendar year is accompanied by the onset of the rainy season and West African Monsoon, with the first substantial rain events occurring in April. The southward retreat of the ITCZ marks the dry season in the Sahel starting in October or November. Recent maps of African soils based on surface reflectance suggest that soils across the Sahel tend to have pHs largely near neutral, but can be higher than 9 in some areas (Vågen *et al*., 2016). The combination of seasonal rainfall variability and soils with neutral or alkaline pHs suggests that Sahelian soils may be an important source of NH_3 at the onset of the rainy season. Although the Sahel has regions of relatively dense cropland, it is characterized by lower levels of fertilizer inputs (FAO, accessed 2018) and smaller loads of atmospheric N deposition (Dentener *et al*., 2006; Galy-Lacaux and Delon, 2014; Laouali *et al*., 2012; though deposition can be elevated at the Sahel's southern boundary) than other parts of the world. However, it

Deleted: .

Deleted: As such, the Sahel is a good region to focus on in determining whether Birch effect NH_3 pulsing is an important process at broad regional scales.

Deleted: The onset of the rainy season is accompanied by rapid mineralization of nitrogen following the wetting of dry soils in East Africa (Semb and Robinson, 1969), and soil NH_3 emission have been shown to be higher at a site in northern Senegal following a rain event (Delon et al., 2017).

Deleted:)

Deleted: ,

4

has moderately high livestock densities (Robinson *et al*., 2014), potentially providing sites of abundant available N for the production of NH_3. Indeed, soil NH_3 emissions have been shown to be higher at a site in northern Senegal following a rain event (Delon *et al*., 2017).

Earlier work using total column observations from the GOME instrument presented evidence of high atmospheric concentrations of nitrogen dioxide (NO_2) over the Sahel in the early rainy season of 2000, which appeared to broadly correspond to rainfall events in the region (Jaeglé *et al*., 2004). These early growing season increases in tropospheric NO_2 concentrations could not be attributed to lightning or to biomass burning, leaving soil emissions the presumed source. Soils emit NO through a variety of biotic and abiotic mechanisms; in the atmosphere, NO rapidly interconverts to NO_2, and the two gases are collectively referred to as NO_x. Inverse modelling subsequently suggested that soil emissions of NO across sub-Saharan Africa were of the same magnitude as emissions from biomass burning, which previously had been thought to be the dominant NO_x source in the region. Note that in this paper, NO is used in discussions of soil emissions specifically. Since satellite observations are of NO_2, we use NO_2 when discussing those observations, and NO_2 or NO_x when discussing modelled surface emissions based on those observations.

At regional scales, the processes controlling seasonal variability in emissions, and the magnitude of emission responses to these controls, are not well constrained. Atmospheric models often rely on static emissions inventories of NH_3 that lack intra-annual variability or detailed environmental controls over emissions from soils (e.g., Bouwman *et al*., 1997; European Commission, Joint Research Center (JRC)/Netherlands Environmental Agency (PBL), 2011; Lamarque *et al*., 2010), particularly for natural ecosystems (e.g., Paulot and Jacob, 2014). Fire emission inventories are generally created using data on burned area, fuel load, combustion completeness to compute dry matter of carbon losses, and emission factors that translate these into trace gas or aerosol emissions, producing daily emissions estimates at 0.25° resolution (e.g., van der Werf *et al*., 2017). Inventories of NH_3 emissions from natural soils tend to rely on a global estimate for the year 1990 (Bouwman *et al*., 1997) and agricultural emission inventories

Deleted: modeling

Formatted: Subscript

Formatted: Subscript

Formatted: Subscript

Formatted: Subscript

with sub-annual temporal resolution tend not to consider environmental controls other than temperature and wind speed (e.g., Paulot and Jacob, 2014).

Here we use satellite retrievals of atmospheric NH_3 concentrations (Whitburn *et al.*, 2016) over Africa to evaluate whether the onset of the rainy season causes pulsed emissions of NH_3 over the Sahel, focusing on the year 2008, and evaluate its environmental drivers. We compare the seasonal pattern in atmospheric NH_3 concentrations observed by satellite to monthly surface NH_3 deposition measured at 7 sites in north equatorial Africa. We also use a simple box model to calculate surface fluxes based on retrieved atmospheric concentrations, and compare modeled surface fluxes to NH_3 emissions from biomass burning as quantified in the Global Fire Emissions Database 4s (GFED4s; van der Werf *et al.*, 2017). Finally, we also make comparisons to modeled surface fluxes of NO_2 derived from NO_2 observations made by the Ozone Monitoring Instrument (OMI; Krotkov, accessed 2018).

2. Methods

2.1 Satellite products

The Infrared Atmospheric Sounding Interferometer (IASI-A), launched aboard the European Space Agency's MetOp-A in 2006, obtains retrievals of atmospheric NH_3 at a global distribution and bi-daily resolution. IASI-A is a polar-orbiting instrument in a sun-synchronous orbit (9:30 Local Solar Time equator crossing, descending node), providing two observations daily; here we use morning observations, when the thermal contrast is more favorable for retrievals (Clarisse *et al.*, 2009; Van Damme *et al.*, 2014). IASI-A provides a horizontal resolution of 12 km over a swath width of about 2,200 km. The retrieval product used follows the approach implemented by Whitburn *et al.* (2016), in which total columns of NH_3 are obtained by calculating a dimensionless spectral index (HRI), which is then converted into a NH_3 total column through the use of a neural network. The neural network uses a range of variables such as temperature and water vapor profiles to represent the state of the atmosphere as best as possible to produce the matching NH_3 total column for that atmospheric state. Retrievals with errors above 100% were excluded from the analysis, though exceptions were made for low concentrations, which tend to have a

5

10

15

20

25

Deleted: x

higher error, when the following condition was met:

Retrieval error × total column NH_3 × 0.01 < 5 ×10^{15} molecules cm^{-2} (1)

where the retrieval error is a percentage and the total column NH_3 is a concentration in molecules cm^{-2}. In addition, only retrievals that were at least 75% cloud-free were used. Given the absence of hourly observations in the Sahel, the detection limit of IASI is difficult to determine with certainty. However, the region experiences high thermal contrast, and IASI seems to be able to reliably observe down to 1 to 2 ppb at the surface (is there a reference for this statement?). We regridded the Level-2 IASI NH_3 product to 0.25° × 0.25° resolution to match the resolution of soil moisture and other data used in the analysis. Specifically, we calculated the concentration for a given grid cell as the mean of all elliptical IASI footprints for which the corners of the grid cell were within the footprint. The IASI product has been validated using ground-based Fourier transform infrared (FTIR) observations of NH_3 total columns, with robust correlations at sites with high NH_3 concentrations, but lower at sites where atmospheric concentrations approach IASI's detection limits (Dammers *et al.*, 2017). Compared to the FTIR observations the IASI total columns are biased low by ~30% which varies per region depending on the local concentrations.

We used the Tropical Rainfall Measuring Mission (TRMM) daily precipitation product (3B42), which is based on a combination of TRMM observations, geo-synchronous infrared observations, and rain gauge observations (Huffman *et al.*, 2007). Independent rain gauge observations from West Africa have been used to validate the product, with no indication of bias in the product (Nicholson *et al.*, 2003).

We used the European Space Agency's Climate Change Initiative (ESA-CCI) 30-year daily soil moisture product gridded at 0.25° × 0.25° resolution (Dorigo *et al.*, 2017; Gruber *et al.*, 2017; Liu *et al.*, 2012). The product is based on both passive and active microwave sensors, and has been validated globally (Dorigo et al., 2014) and in East Africa (McNally *et al.*, 2016). Although the product exhibited

moderate correlation with ground observations globally, it provides relatively high correlations (r~0.7) for West African sites when seasonality is included in the analysis (Dorigo *et al*., 2014).

We also used the publicly available level 3 tropospheric NO_2 concentrations product from OMI, a nadir-viewing spectrometer measuring solar backscatter in the UV-visible range aboard NASA's Aura satellite (Krotkov *et al*., 2017). The product is cloud-screened, including only pixels that are at least 70% cloud-free, and provided in at 0.25° × 0.25° resolution. The OMI product relies on air mass factors calculated with the assistance of an atmospheric chemical transport model, and is sensitive to model representations of emission, chemistry and transport data. These are generally poorly constrained for regions not commonly analyzed in chemical transport models such as sub-Saharan Africa (McLinden *et al*., 2014). Additional bias may be introduced due to the reliance on nearly cloud-free pixels, where greater sunlight may induce higher photochemical rates. For example, the current product is biased roughly 30% low over the Canadian oil sands (McLinden *et al*., 2014). Level 2 OMI-NO_2 product has been validated against in situ and surface-based observations showing good agreement (Lamsal *et al*., 2014). In statistical analyses, soil moisture, precipitation, and NO_2 data were masked to match pixels for which NH_3 retrievals were also available.

2.2 Surface flux calculations

A range of possible surface fluxes of NH_3 and NO_2 from our focal study region in the Sahel, ranging from 10°N to 16°N and from 0°E to 30°E, were calculated from IASI total column NH_3 concentrations and OMI-NO_2 tropospheric concentrations using a simple box model (Jacob, 1999). The specific region was selected as representative of the Sahel, and to allow for direct comparisons to earlier work examining NO_2 emissions from the region (Jaeglé *et al*., 2004). Daily mean gridded concentrations of retrievals for each gas were averaged across the focal region with units of molecules cm^{-2}. The mean total column concentrations of gas *x* were converted to a mean surface density for the region in units of kg m^{-2} for each day, using the following equation:

$$M_{x,t} = (TC_{x,t} \times MM_x \times 10)/N_a \tag{2}$$

8

where $M_{x,t}$ is the mean surface density of gas x for day t, $TC_{x,t}$ is the average of retrieved total columns of gas x in units of molecules cm^{-2} for day t, MM_x is the molar mass of gas x, and N_a is Avogadro's number. The dividend on the right hand of the equation is multiplied by 10 to convert the mean surface density to units of kg m^{-2}. This mean surface density was then used in the box model to calculate a mean surface flux for each day, assuming first order losses of gas x:

$$E_{x,t}(mol) = \frac{(M_{x,t} - M_{x,t-d}e^{-d/\tau_x})}{\tau_x(1 - e^{-d/\tau_x})} \qquad (3)$$

where $E_{x,t}$ is the surface flux on day t in units of kg m^{-2} day^{-1}, d is the time between subsequent observations (one day in this study), and τ_x is the effective lifetime of a molecule of gas x, including both reactive and transport losses. As both the effective lifetime and the surface flux are unknowns in the equation, we use a range of plausible lifetimes for each gas to calculate a range of surface fluxes. For NH_3, we use lifetimes of 6, 12, 24, and 36 hours (Dentener and Crutzen, 1994; Whitburn $et\ al.$, 2015); for NO_2, we use lifetimes of 6, 12, and 24 hours (Beirle $et\ al.$, 2011; de Foy $et\ al.$, 2015; Jena $et\ al.$, 2014). The values were selected to reflect the possible range of lifetimes throughout the year, including periods of elevated wet deposition during the rainy season. Our box modelled NO_2 emissions used only satellite observations for grid cells where NH_3 observations were also present; model results restricted to using satellite observations for grid cells where both NH_3 and NO_2 are presented in the supplemental information.

2.3 Emissions inventory

GFED4s (van der Werf $et\ al.$, 2017) provides monthly fire emissions at 0.25° resolution based on satellite-derived burned area (Giglio $et\ al.$, 2013; Randerson $et\ al.$, 2012) and a modified version of the Carnegie-Ames-Stanford-Approach (CASA) biogeochemical model (Potter $et\ al.$, 1993). Daily emissions are calculated using data on the fraction of monthly emissions emitted on each date. Uncertainty in GFED fire emissions stems from uncertainty in burned area, fuel consumption, and emission factors but is poorly

constrained. According to van der Werf *et al.* (2017) a 1σ of about 50% for fire carbon emissions is reasonable for continental scale estimates. This may also be a best-guess estimate for fire NH_3 emissions in our study region; while the uncertainty in NH_3 emission factors is large because few fires have been sampled and adds to the total uncertainty, burned area and fuel consumption in savannas are, in general, better constrained than in other biomes.

2.4 Statistical analyses

Pearson product moment correlation analyses were conducted using pearsonr from the scipy.stats package in Python v3.6.3.

3. Results and Discussion

The wetting of dry soils has been known to stimulate biogeochemical cycling since at least the 1950s. Its role in creating large pulsed emissions of trace gases such as CO_2 and NO has been demonstrated at laboratory (e.g., Birch and Friend, 1956), field (e.g., Davidson, 1992), and regional scales through satellite observations (Jaeglé *et al.*, 2004) and observation networks (Adon *et al.*, 2010). Evidence for its importance to emissions of NH_3 has been limited to a few laboratory and field studies, with sometimes contrasting results, and its importance at landscape or regional scales is not well constrained. Here we present evidence that the Birch effect is an important driver of NH_3 emissions at regional scales, and likely responsible for the periods of the highest atmospheric NH_3 concentrations over the Sahel region in Africa.

3.1 Seasonal variability in NH_3 concentrations over Africa

Atmospheric NH_3 concentrations in 2008 exhibited broad seasonality that appears to correspond to seasonal precipitation patterns across the continent (Figure 1). In January, mean monthly concentrations are highest across a latitudinal band from roughly 5°N to 10°N, broadly corresponding to the region of highest biomass burning emissions (Figure 1). In April, higher cumulative monthly precipitation across the southern Sahel coincides with increased mean monthly NH_3 concentrations in the

10

Deleted: is

Deleted: 2

focal region (the red box in Figure 1b); fire emissions are generally absent across the Sahel and much of the rest of the continent in April, with some emissions occurring along coastal West Africa. By August, during the middle of the West African Monsoon, hotspots of ammonia concentrations are generally absent from the continent, though concentrations are slightly elevated in central southern Africa, where
5   emissions from biomass burning are also elevated (Figure 1).

3.2 Evidence for precipitation-induced emissions of NH$_3$ in the Sahel

For our focal region of the Sahel (defined above and outlined in red in Figure 1), mean atmospheric
10   NH$_3$ concentrations exhibit two distinct peaks in late March and April (Figure 2a, highlighted in light and dark pink, respectively), which represent the highest concentrations observed in 2008. The late March peak occurs at the same time as an apparent modest increase in mean soil moisture (Fig 2b). The peak in April, during which atmospheric NH$_3$ concentrations over the Sahel are elevated relative to other parts of north equatorial Africa (Figure 3a), occurs during the first period of sustained rainfall in the focal region,
15   and corresponds to a peak in soil moisture, suggesting a possible causal relationship between changes in soil moisture and atmospheric NH$_3$ concentrations (Figure 2b and section 3.2.1 below). This increase does occur following a possible modest increase in mean fire emissions (Fig 2a) across the Sahel. Overall, however, the seasonality in IASI-retrieved atmospheric NH$_3$ concentrations exhibits a marked difference from the seasonality in GFED4s NH$_3$ emissions from fires, which start increasing in September and peak
20   in November (Fig 2a and section 3.2.2 below).

3.2.1 Soil moisture controls over early growing season atmospheric NH$_3$ concentrations

Multiple lines of evidence support a causal relationship between changes in soil moisture and atmospheric NH$_3$ concentrations across the Sahel. Foremost are the significant correlations between
25   ESA-CCI's soil moisture product and the IASI total column during the onset of the rainy season. Specifically, for the period from February 23 to May 1, 2008, there is a significant correlation between mean atmospheric NH$_3$ concentrations of all pixels with acceptable retrievals in the Sahel focal region and mean soil moisture across the same set of pixels (r=0.28, P=0.02; Figure 4a). This correlation

11

integrates all pixels across the Sahel, and thus excludes any sub-regional spatial structure in the data. To examine whether a relationship between soil moisture and NH_3 concentrations is also present at a finer spatial scale, we conducted a correlation between the two variables for each pixel for which both variables were present during April, and again found a significant positive linear correlation ($r=0.16$, $p<0.001$;

5 Figure 4b). Maps of 3-day averages for precipitation, soil moisture, and total column NH_3 concentration over the southern Sahel at 0.25° resolution illustrate the changes in each variable that occur during the development of the April emissions peak (Figure 5). Between April 13 and April 27, precipitation events in the southern half of the focal region (left-hand column) appear to be accompanied by steady increases in soil moisture (middle column) and total column NH_3 (right-hand column).

10

Although the explanatory power of the correlations between ESA-CCI's soil moisture product and the IASI total column NH_3 concentrations is relatively low, it demonstrates a broad regional correlation between NH_3 concentrations and changes in soil moisture at the onset of the rainy season – a relationship that is strong enough to be observed at the scale of the Sahel. To provide some context for the statistical

15 result, earlier work finding that rainfall is responsible for large emissions of NO_2 in the same region did not include any statistical analysis in support of its findings (Jaeglé *et al.*, 2004), and studies using satellite observations to infer environmental controls interpret correlation coefficients on the order of 0.25 to be evidence of a strong effect (e.g., Andela *et al.*, 2017). Additionally, we would not necessarily expect a linear relationship between the quantity of soil moisture and the quantity of NH_3 emitted.

20

3.2.2 Minimal contribution of fire emissions to early growing season pulses

We can further exclude biomass burning as the source of the observed pulses of atmospheric NH_3. Biomass burning occurs in the Sahel with a well-known seasonality as based on several

25 independent satellite fire metrics such as burned area and active fire detections (Duncan, 2003; Giglio *et al.*, 2006). In general, burning in the Sahel occurs in the second half of the year, and few emissions are expected at the onset of the rainy season (Figure 1, 2). A comparison between our simple box model estimates of NH_3 flux and emissions from the GFED4s inventory strongly supports the hypothesis that

12

biomass burning does not play an important role in NH_3 emissions during March or April, and further suggests that biomass burning may represent a relatively unimportant regional source of NH_3 during most of the year, outside of the biomass burning season (Figure 6). The modelled total surface flux based on IASI observations varies depending on the effective lifetime used by up to a factor of roughly 4, with seasonal patterns mirroring the patterns in atmospheric concentration, and the largest emissions occurring during the pulses in March and April (Figure 6). In contrast, fire emissions of NH_3 from GFED4s are concentrated in the second half of the year, and are negligible during March and April, suggesting that they do not contribute to the early growing-season emission pulses.

The importance of a source of NH_3 other than biomass burning in equatorial North Africa was suggested earlier for 0 to 10° N, a region immediately south of the Sahel and of the southern boundary of our focal region in Figures 1 and 2 (Van Damme *et al.*, 2015; Whitburn *et al.*, 2015). Whitburn *et al.* observe a one to two-month lag between peak fire radiative power and IASI- NH_3 that differs from the pattern of IASI carbon monoxide (CO) concentrations, suggesting that fire emissions can explain only some of the atmospheric NH_3 present. They speculate that soils may be the source of NH_3 emissions following the fire season, perhaps resulting from an increase in volatilization caused by increasing soil temperatures and pH, though the paper is focused on evaluating fire emissions and they do not test this hypothesis (Whitburn *et al.*, 2015). Van Damme *et al.* speculate that the emissions are agricultural in nature (Van Damme *et al.*, 2015). IASI-NH_3 concentrations in the other regions examined (southern Africa, Southeast Asia, and central South America) generally track fire activity, or are thought to be due to anthropogenic emissions (Whitburn *et al.*, 2015). Although we have focused on the Sahel, it seems possible that the seasonality of rainfall in environments further south, between 0°N and 10°N, could partly explain the elevated emissions observed there following the end of the fire season.

3.2.3 Co-emission of NH_3 and NO_2

The peak in NH_3 concentrations in April occurs at the same time as a peak in NO_2 concentrations (though unlike NH_3, the April peak does not represent the highest annual atmospheric

13

concentration of NO_2). For the month of April, total column NH_3 concentrations and tropospheric NO_2 concentrations integrated across the entire focal region are strongly correlated (r=0.78, p<0.0001). This simultaneous increase in atmospheric NO_2 and NH_3 concentrations provides additional, indirect support for a soil source of NH_3 (Figure 2, 6). In addition to abundant field- and laboratory evidence that

5 previously dry soils emit large pulses of NO following wetting (Davidson, 1992; Davidson *et al.*, 1991; Dick *et al.*, 2001; Meixner *et al.*, 1997), Jaegle *et al.* (2004) showed that this soil NO pulse is responsible for the highest concentrations of atmospheric NO_2 over the same region we focused on. As with the seasonal pattern in NH_3 concentrations, seasonal variation in OMI-NO_2 tropospheric concentrations does not match that of the GFED4s NO_2 emissions from fires (Figure 6). We believe that the simplest

10 explanation for our box model results showing the strong correlation between tropospheric NO_2 and total column NH_3 concentrations in April is that the two pulses are the result of soil emissions triggered by the same environmental change—in this case, an increase in soil moisture following an extended dry period.

Like NH_3, concentrations of NO_2 also exhibit a peak in mid-March, but the peak lags a week

15 behind the NH_3 peak (Figure 2). Although NO emissions from soils can peak within hours after wetting (Davidson, 1992), in a laboratory setting using soils from the Mojave Desert, an NO pulse lagged 1 to 2 days behind an NH_3 pulse following experimental wetting (McCalley and Sparks, 2008). The authors argue that this lag may be related to competition for NH_4^+ between NH_3 volatilization and nitrification, with volatilization generally outcompeting nitrification during the initial period following wetting. An

20 alternative or additional contributing factor to the lag may be related to the population dynamics of nitrifying bacteria. Although the transcriptional response of nitrifiers to wetting can be very rapid (Placella and Firestone, 2013), at a population level nitrifiers are generally slow-growing (Robertson and Groffman, 2007), suggesting that populations in resource-limited environments may not be able to immediately take advantage of sudden large increases in resource availability. For example, NO emission

25 responses to inorganic N inputs—which arguably provides a similar immediate release from a resource limitation as wetting of dry soils for nitrifiers, particularly in relation to the presumed increase in NH_4^+ concentrations caused by wetting—exhibited pulse responses that lagged roughly a week behind fertilizer additions in Kenya (Hickman *et al.*, 2017). In the case of the Sahel, nitrifier populations may not be able

14

to recover quickly from the extended dry conditions in March, and a lagged emission response of NO could be explained by the slow population-level response to the flush of mineralized N that follows wetting.

The March NO_2 peak is also smaller than the April NO_2 peak, and smaller than the April NH_3
5 peak. Field studies have observed larger pulses following the second rainfall of the season (Meixner *et al.*, 1997). The initial increase in soil moisture during March was modest (Figure 2), so it seems possible that soils dried out quickly, before populations of nitrifying bacteria grew large enough to trigger an NO pulse of the magnitude that occurs in April. Increased competition for available NH_4^+ by nitrifying bacteria in April may have limited the NH_3 pulse.

10 There is also a clear mis-match in the timing of the peak NH_3 concentrations, which occurred in March and April, and peak NO_2 concentrations, which occurred in May and June (Figure 2). We believe that several factors are likely contributing to the different temporal dynamics of NH_3 and NO_2 concentrations. First, to be clear, we argue that the rainfall events in March and April are indeed triggering pulses of both gases, illustrated in part by the strong correlation between the two gases during April
15 (r=0.78, p<0.0001; Figure 2; for a strict comparison in which concentrations of NO_2 and NH_3 are calculated using only grid cells that have observations for both gases, see Figure S1, though the results are qualitatively similar to Figure 2). Temporal patterns of surface NO_2 concentrations observed by the INDAAF network may also support the presence of these smaller, early pulses (Figure S2). Although not explicitly investigated, we believe earlier studies of NO_2 pulsing in the Sahel that focus on emissions
20 during May and June include observations of similar early season pulses (Jaegle *et al.* 2004, Hudman *et al.* 2012).

The smaller early season NO_2 pulses are potentially the result of the nitrifier population dynamics alluded to above. Specifically, because population growth is slow, nitrifying populations are smaller during March and April than they will become later in the growing season when they are released from
25 sustained environmental limitations on growth, and so nitrification rates remain lower in these early responses. In an earlier field study conducted in Davis, California, which also experiences distinct dry and rainy seasons, nitrifier population growth rates were very slow to respond to ammonium additions, roughly matching the temporal patterns of NO_2 emissions we observed in the Sahel (Okano *et al.* 2004).

15

In that study, population size did not increase during the first week following ammonium sulfate applications, and then rose by roughly 50% in the second week. Between the 13th and 39th day, however, the population roughly tripled. In the Sahel, nitrifying populations are presumably released from widespread water limitation around the beginning of May (Figure 2), and NO$_2$ concentrations grow to their maximum a little more than a month later. An additional point is that although the pulsing behaviour of NH$_3$ appears to diminish in May and June, total emissions during those months are almost as elevated relative to the dry period as emissions during March and April (167 mg N m^{-2} and 173 mg N m^{-2} for each 61-day period, respectively; Figure 6). Consequently, it could be argued that May and June remain important months for both NO$_2$ and NH$_3$ emissions. For a presentation of modelled emissions calculated based only grid cells that have satellite observations for both gases, see Figure S3. This additional screening reduces annual modelled NH$_3$ emissions by roughly 5%, and reduces modelled emissions during the pulses by roughly 2-3% relative to modelled NH$_3$ emissions that do not take the presence or absence of NO$_2$ observations into account.

A second point is that both NH$_3$ volatilization and nitrification are dependent on NH$_4^+$ availability, and thus competition between these processes for NH$_4^+$ is likely to contribute to the observed temporal dynamics of atmospheric NH$_3$ and NO$_2$ concentrations. The increased competition for available NH$_4^+$ from growing nitrifier populations could contribute to the observed decline in NH$_3$ emissions between April and May. Earlier researchers have hypothesized that competition between NH$_3$ volatilization and nitrification for NH$_4^+$ is so extreme that the two processes cannot occur at the same time (Praveen-Kumar and Aggarwal, 1998). However, soil emissions of NO and NH$_3$ have been shown to be broadly coupled in the Sahel (Delon *et al.* 2018), and the few field and lab studies measuring soil emissions of both gases following wetting observe positive fluxes of each (McCalley and Sparks, 2008; Schlesinger and Peterjohn, 1991; Soper *et al.*, 2016), with NH$_3$ dominating emissions from desert soils (McCalley and Sparks, 2008; Schlesinger and Peterjohn, 1991) and NO$_2$ dominating from grassland soils (Soper *et al.*, 2016). Our findings contrast with those of Soper *et al.*, as NH$_3$ appears to be the dominant species emitted during pulse events in March and April (Figure 6). We expect that even were the two processes mutually exclusive at the scale of a soil core or chamber, heterogeneity in soil properties at the pixel or regional scale would explain our observations of coinciding peaks of NO$_2$ and NH$_3$.

16

3.3 Magnitude and importance of soil NH$_3$ emission pulses

5   During the early growing season, atmospheric concentrations of NH$_3$ are roughly an order of magnitude higher than NO$_2$ (Figure 2). It is important to note that NH$_3$ retrievals generally have a higher error, and that our screening process may introduce a potential bias in that we permit retrievals with higher uncertainty if they are low concentrations; we also retain observations of negative concentrations. In addition, as mentioned earlier, compared to FTIR observations the IASI total

10   columns are biased low by ~30% which varies per region depending on the local concentrations. From this perspective, our concentration and emission estimates can be considered conservative.

Because the magnitude of mean surface fluxes depends on the effective lifetime used in the simple box model, comparisons between the modelled fluxes of NO$_2$ and NH$_3$ are not straightforward. It is also

15   important to note the simplifying assumption of a uniform atmospheric profile in the box model, which ignores any variation in vertical distribution. Still, we believe a uniform profile is a reasonable assumption, especially for soil fluxes. Each of these gases has relatively short lifetimes, and unlike fire plumes, are unlikely to be rapidly lofted to high altitudes following emission from soil. In addition there is very little variation in NH$_3$ distribution throughout the boundary layer in the assumed IASI profile. In

20   general, our modelled emissions suggest that NH$_3$ is probably emitted at substantially higher rates from soils than NO during pulse events (Figure 6). This result is unexpected, given earlier observations that NH$_3$ tends to be the dominant source in highly alkaline desert soils (pH 9-11; McCalley and Sparks, 2008), whereas emissions from grassland soils with a more neutral pH, as might be expected in the Sahel, were dominated by NO, by roughly a factor of 10:1 (Soper *et al.*, 2016). This pulse produces NH$_3$

25   concentrations comparable in magnitude to the peak concentrations over many of the Earth's major biomass burning regions (Whitburn *et al.*, 2015). Indeed, NH$_3$ emissions during the date range February 29-March 16 and April 12-May 1, which cover the two emission peaks during that period, represented about one fifth of annual NH$_3$ emissions from our focal region in the Sahel (annual emissions of ~0.4 to

---

Deleted: A second potential factor involves the timing of precipitation events early in the rainy season. One reason Birch Effect N trace gas emissions occur is the sudden flush of inorganic nitrogen made available by the lysing of microbes from the sudden change in soil moisture and osmotic potential. Small early rainy season precipitation events may be substantial enough to promote rapid population growth of soil microbes. If these early season events are followed by a drying of soils, or if later precipitation events¶

Deleted: Although earlier researchers have hypothesized that NH$_3$ volatilization and nitrification cannot co-occur in the same soils (Praveen-Kumar and Aggarwal, 1998), the few field and lab studies measuring soil emissions of both gases following wetting observe positive fluxes of each (McCalley and Sparks, 2008; Schlesinger and Peterjohn, 1991; Soper et al., 2016), with NH$_3$ dominating emissions from desert soils (McCalley and Sparks, 2008; Schlesinger and Peterjohn, 1991) and NO$_2$ dominating from grassland soils (Soper et al., 2016). We expect that even were the two processes mutually exclusive at the scale of a soil core or chamber, heterogeneity in soil properties at the pixel or regional scale can explain our observations of coinciding pulses of NO and NH$_3$.¶

Formatted: Font: Times New Roman, 12 pt, English (US)

Deleted:

Formatted: Font: Font color: Auto

Deleted: however,

Deleted: , possibly by a factor of ten or more

2 Tg N, and total pulse emissions of ~0.1 to 0.5 Tg N, depending on the effective lifetime assumed, but assuming that the mean effective lifetime during the pulses is equal to the mean effective lifetime throughout the year). It is important to note that in addition to uncertainty associated with the NH_3 retrievals, additional sources of bias and uncertainty—such as the use of an effective lifetime rather than explicitly accounting for deposition fluxes and chemistry, uncertainty in the value and variability in that lifetime, and biases in both the IASI and OMI retrievals—limit our ability to quantitatively constrain the surface NH_3 or NO_2 fluxes, or to make strict quantitative comparisons between them.

Within the Sahel, the March and April pulses are responsible for the highest concentrations of atmospheric NH_3 during 2008. The magnitude of NH_3 emissions during theses pulses are of a similar magnitude as emissions from biomass burning in north equatorial Africa (Whitburn *et al.* 2015). This substantial pulse of NH_3, and the co-occurrence of a pulse of NO_x, could be an important source of $PM_{2.5}$ in the region during the first half of the year. Secondary inorganic aerosols such as ammonium sulfate are formed in reactions involving NH_3, and ammonium nitrate aerosol formation requires both gaseous NH_3 and NO_x. In the Sahel, combustion sources of NO_2 are relatively small in March and April (Fig. 6), making soil NO emissions potentially more important in the formation of $PM_{2.5}$.

3.4 Comparison to surface observations

The INDAAF network (International Network to Study Deposition and Atmospheric Chemistry in Africa, http://www.indaaf.obs-mip.fr) provides monthly surface NH_3 deposition rates between 1998 to 2016 for seven sites in north equatorial Africa, both in and outside the Sahel. The work of Adon *et al.* (2010) presents an analysis of annual and seasonal variability of surface gases concentrations including NO_2 and NH_3 from the long-term monitoring INDAAF stations over the period 2000-2007. The sites in the Sahel (Agoufou, Mali, Banizoumbou, Niger, and Katibougou, Mali; figures 3b, 3c, and 3f, respectively) exhibit broadly similar seasonal patterns, with NH_3 concentration increases starting in April (or March in the 2008 case of Katibougou, Mali; Figure 3f), but this seasonal pattern is generally absent in sites outside the Sahel (Figure 3d, 3e, 3g, and 3h). These seasonal patterns are broadly consistent with the pulsing dynamics observed by IASI in the Sahel, and the absence of pulsing outside

18

Deleted: x

Deleted: (

Deleted: ,

Deleted: HNO_3, O_3, SO_2, and

Deleted: The two sites in the Sahel (Figure 3c (Banizoumbou, Niger) and 3f (Katibougou, Mali))

Deleted: (

Deleted:)

Deleted: 3b,

the Sahel (Figure 3), though the peak concentrations observed at the surface tend to occur later than those observed by satellite in Banizoumbou and Katibougou.

The difference in the timing of peak NH_3 concentrations between the IASI observations and surface observations at Banizoumbou and Katibougou may be because of random variation and the effects of local influences, which are likely also responsible for variation among the three sites. In addition, deterministic variation in NH_3 emissions in the Sahel is likely important. These sites are located at latitudes near the northern boundary of our focal area, and could be influenced by emissions from the north. In addition, we observe a north-south gradient in soil moisture, precipitation, and NH_3 concentrations during the pulse event in April (Figure 4), suggesting that pulsing is larger in the southern part of our focal area during this period. The onset of the rainy season tends to occur later in more northern latitudes, which would be consistent with higher NH_3 concentrations observed later in the year in Banizoumbou and Katibougou. Indeed, IASI observations of 1° gridcells over each of the three INDAAF sites show better agreement with the surface observations, with peak NH3 concentrations occurring in May for all sites during 2008 (Figure S4).")

Other factors may contribute to variation in NH_3 concentrations observed across all the INDAAF sites. An earlier evaluation of seasonal patterns in the surface observation network found that emission patterns differ between wet savannah and dry savannah: dry season emissions tend to be higher in wet savannah, where biomass burning dominates annual emissions (Adon *et al*., 2010). In dry savannah ecosystems, emissions are higher during the wet season, and are likely enhanced by the volatilization of N inputs from agro-pastoralism in the region, leading to high total N deposition fluxes (Adon *et al*., 2010). It is conceivable that regional differences in soil pH (Vågen *et al*., 2016) could also result in different rates of soil NH_3 emissions. In addition, higher leaf area index in wet savannahs and forest could result in more interception of NH_3, reducing soil contributions to atmospheric concentrations during the wet season.

3.5 Later growing season NH_3 emissions

19

After the early season pulses, NH$_3$ concentrations and fluxes remain fairly elevated (Figure 2, 6); during this period of May through July, NO$_2$ concentrations and fluxes increase, becoming closer in magnitude to NH$_3$ (Figure 2, 6). This pattern is consistent with earlier studies describing elevated concentrations of these gases in or near our focal study region for several months following the end of the biomass burning season (Jaeglé *et al.*, 2004; Whitburn *et al.*, 2015). Jaegle *et al.* (2004) attribute these elevated concentrations to the wetting of dry soils, and Whitburn *et al.* (2015) to increasing surface temperatures and the possible acidification of soils. The mean start of the cropping season ranges from May to August in the focal region, based on NDVI-based observations of plant phenology (Vrieling *et al.*, 2011), suggesting that the bulk of elevated NO$_2$ and NH$_3$ in our modeled emissions occur after planting, and well into the rainy season. Elevated emissions could be associated with soil disturbance from tillage (e.g., Yang *et al.*, 2015) or from the use of fertilizer inputs, which have been argued to be higher than generally acknowledged in the scientific and development literature (Cobo *et al.*, 2010; Sheahan and Barrett, 2017), though N additions in Sahelian countries such as Niger tend to be very low, even for farmers who use fertilizer (Masso *et al.*, 2017; Sheahan and Barrett, 2017).

3.6 Possible sources of error and bias

It is worth noting that the morning overpass time used in this analysis is likely to cause a further underestimation of daily NH$_3$ concentrations, as emissions would be expected to follow diurnal temperature variation and be higher in the afternoon (Van Damme *et al.*, 2015). A more sophisticated inverse modelling approach (e.g., using a Bayesian approach in combination with an atmospheric chemical transport model) could provide firmer insight into the magnitude of emissions, as well as provide some insight into the magnitude of specific NH$_3$ sources. Our analysis is subject to several additional sources of uncertainty: increased cloud cover during the rainy season tends to result in fewer observations than during the dry season, so our regional means are based on different numbers of observations at different times of year.

Although the explanatory power of the linear relationship between soil moisture and emissions in the early part of the rainy season is relatively low, this would be expected in part due to the complex

Deleted: comparable

Deleted: in the region

processes which vary over time. Multiple studies have shown that rewetting of dry soils results in lower emission pulses for the same level of water addition (Davidson, 1992; Davidson *et al.*, 1991), including of NH_3 emissions (Soper *et al.*, 2016). It also seems plausible that there are threshold effects in which an initial increase in soil moisture may simply need to be large enough to activate dormant microbial communities and/or cause a flush of labile microbial N to trigger an emissions pulse, such that the pulse response might best be described with a piecewise function. Asynchrony between plant and microbial activity during soil wet up and dry down (Collins *et al.*, 2008), and different activation thresholds for microbial and plant responses to precipitation (Dijkstra *et al.*, 2012) may also play a role in determining the amount of available NH_4^+ for volatilization at different times in the early rainy season.

3.7 Conclusion

Satellite measurements of trace gases—although not without their limitations—provide a powerful tool for understanding global and regional atmospheric composition, and for gaining insights into the controls over nitrogen cycling and trace gas emissions, particularly for regions where other types of measurements are scarce. With daily and global coverage and additional satellite observed variables such as precipitation, soil moisture, biomass burning emissions, and tropospheric NO_2 concentrations, it is possible to evaluate specific mechanisms behind the seasonality of trace gas emissions. In an evaluation of the Sahel during 2008, we find that NH_3 concentrations are elevated during March and April, a period when biomass burning emissions are absent, but when tropospheric NO_2 concentrations exhibit similar temporal dynamics. We further find that the increase in NH_3 concentrations is positively correlated to changes in soil moisture at the start of the rainy season. Using a simple box model, we estimate that average emissions for the entire Sahel are between 2 and 6 mg NH_3 m^{-2} day^{-1} during peaks of the observed pulses, though note that these estimates are subject to substantial bias and uncertainty. We conclude that the Birch effect is an important and geographically broad driver of NH_3 emissions, and an important component of the N cycle in the Sahel.

References

Adon, M., Galy-Lacaux, C., Yoboue, V., Delon, C., Lacaux, J. P., Castera, P., Gardrat, E., Pienaar, J., Ourabi, Al, H., Laouali, D., Diop, B., Sigha-Nkamdjou, L., Akpo, A., Tathy, J. P., Lavenu, F. and Mougin, E.: Long term measurements of sulfur dioxide, nitrogen dioxide, ammonia, nitric acid and ozone in Africa using passive samplers, Atmos. Chem. Phys., 10, 7467–7487, doi:10.5194/acp-10-7467-2010, 2010.

Andela, N., Morton, D. C., Giglio, L., Chen, Y., van der Werf, G. R., Kasibhatla, P. S., DeFries, R. S., Collatz, G. J., Hantson, S., Kloster, S., Bachelet, D., Forrest, M., Lasslop, G., Li, F., Mangeon, S., Melton, J. R., Yue, C. and Randerson, J. T.: A human-driven decline in global burned area, Science, 356, 1356–1362, doi:10.1126/science.aal4108, 2017.

Anderson, I. C. and Levine, J. S.: Relative rates of nitric oxide and nitrous oxide production by nitrifiers, denitrifiers, and nitrate respirers, Applied and Environmental Microbiology, 51(5), 938–945, 1986.

Austin, A. T., Yahdjian, L., Stark, J. M., Belnap, J., Porporato, A., Norton, U., Ravetta, D. A. and Schaeffer, S. M.: Water pulses and biogeochemical cycles in arid and semiarid ecosystems, Oecol., 141(2), 221–235, doi:10.1007/BF00335913, 2004.

Beirle, S., Boersma, K. F., Platt, U., Lawrence, M. G. and Wagner, T.: Megacity emissions and lifetimes of nitrogen oxides probed from space, Science, 333(6050), 1737–1739, doi:10.1126/science.1207824, 2011.

22

Bergstrom, A.-K. and Jannson, M.: Atmospheric nitrogen deposition has caused nitrogen enrichment and eutrophication of lakes in the northern hemisphere, Global Change Biol., 12, 635–643, doi:10.1111/j.1365-2486.2006.01129.x, 2006.

Birch, H. F.: The effect of soil drying on humus decomposition and nitrogen availability, Plant Soil, 10, 5 9–31, 1958.

Birch, H. F.: Nitrification in soils after different periods of dryness, Plant Soil, 12, 81–96, 1960.

Birch, H. F. and Friend, M. T.: Humus decomposition in East African soils, Nature, 178, 500–501, 1956.

Bobbink, R., Hicks, K., Galloway, J., Spranger, T., Alkemade, R., Ashmore, M., Bustamante, M., 10 Cinderby, S., Davidson, E. and Dentener, F.: Global assessment of nitrogen deposition effects on terrestrial plant diversity: a synthesis, Ecol. Appl., 20, 30–59, 2010.

Borken, W. and Matzner, E.: Reappraisal of drying and wetting effects on C and N mineralization and fluxes in soils, Global Change Biol., 15, 808–824, doi:10.1111/j.1365-2486.2008.01681.x, 2009.

Bouwman, A. F., Lee, D. S. and Asman, W.: A global high-resolution emission inventory for ammonia, 15 Global Biogeochem. Cy., 11, 561–587, 1997.

Clarisse, L., Clerbaux, C., Dentener, F., Hurtmans, D. and Coheur, P.-F.: Global ammonia distribution derived from infrared satellite observations, Natur Geosci., 2, 479–483, doi:10.1038/ngeo551, 2009.

Cobo, J. G., Dercon, G. and Cadisch, G.: Nutrient balances in African land use systems across different spatial scales: A review of approaches, challenges and progress, Agric., Ecosys. Environ., 136, 1–15, 20 doi:10.1016/j.agee.2009.11.006, 2010.

Collins, S. L., Sinsabaugh, R. L., Crenshaw, C., Green, L., Porras-Alfaro, A., Stursova, M. and Zeglin, L. H.: Pulse dynamics and microbial processes in aridland ecosystems, J. Ecol., 96, 413–420, doi:10.1111/j.1365-2745.2008.01362.x, 2008.

Dammers, E., Shephard, M. W., Palm, M., Cady-Pereira, K., Capps, S., Lutsch, E., Strong, K., 25 Hannigan, J. W., Ortega, I., Toon, G. C., Stremme, W., Grutter, M., Jones, N., Smale, D., Siemons, J., Hrpcek, K., Tremblay, D., Schaap, M., Notholt, J. and Erisman, J. W.: Validation of the CrIS Fast Physical NH$_3$ Retrieval with ground-based FTIR, Atmos. Meas. Tech. Discuss., 10, 2645-2667, doi:10.5194/amt-2017-38-AC2, 2017.

30 Davidson, E. A.: Pulses of nitric oxide and nitrous oxide flux following wetting of dry soil: An assessment of probable sources and importance relative to annual fluxes, Ecol. Bull., 149–155, 1992.

23

Davidson, E. A., Vitousek, P. M., Matson, P. A., Riley, R., García-Méndez, G. and Maass, J. M.: Soil emissions of nitric oxide in a seasonally dry tropical forest of México, J. Geophys. Res.- Biogeosci., 96, 15439–15445, doi:10.1029/91JD01476, 1991.

Dawson, G. A.: Atmospheric ammonia from undisturbed land, J. Geophys. Res.-Biogeosci., 82, 3125–
5   3133, 1977.

de Foy, B., Lu, Z., Streets, D. G., Lamsal, L. N. and Duncan, B. N.: Estimates of power plant NOx emissions and lifetimes from OMI NO2 satellite retrievals, Atmos. Environ., 116, 1–11, doi:10.1016/j.atmosenv.2015.05.056, 2015.

Delon, C., Galy-Lacaux, C., Serca, D., Loubet, B., Camara, N., Gardrat, E., Saneh, I., Fensholt, R.,
10   Tagesson, T., Le Dantec, V., Sambou, B., Diop, C. and Mougin, E.: Soil and vegetation-atmosphere exchange of NO, NH3, and N2O from field measurements in a semi-arid grazed ecosystem in Senegal, Atmos. Environ., 156, 36–51, doi:10.1016/j.atmosenv.2017.02.024, 2017.

Delon, C., Galy-Lacaux, C., Serca, D., Personne, E., Mougin, E., Adon, M., Le Dantec, V., Loubet, B., Fensholt, R., and Tagesson, T.: Modelling land atmosphere daily exchanges of NO, NH3, and CO2 in a
15   semi-arid grazed ecosystem in Senegal, Biogeosci. Disc., https://doi.org/10.5194/bg-2018-366, 2018.

Dentener, F. J. and Crutzen, P. J.: A three-dimensional model of the global ammonia cycle, Journal of Atmos. Chem., 19, 331–369, doi:10.1007/BF00694492, 1994.

Dentener, F., Drevet, J., Lamarque, J. F., Bey, I., Eickhout, B., Fiore, A. M., Hauglustaine, D., Horowitz, L. W., Krol, M., Kulshrestha, U. C., Lawrence, M., Galy-Lacaux, C., Rast, S., Shindell, D.,
20   Stevenson, D., Van Noije, T., Atherton, C., Bell, N., Bergman, D., Butler, T., Cofala, J., Collins, B., Doherty, R., Ellingsen, K., Galloway, J., Gauss, M., Montanaro, V., Müller, J. F., Pitari, G., Rodriguez, J., Sanderson, M., Solmon, F., Strahan, S., Schultz, M., Sudo, K., Szopa, S. and Wild, O.: Nitrogen and sulfur deposition on regional and global scales: A multimodel evaluation, Glob. Biogeochem. Cy., 20, GB4003, doi:10.1029/2005GB002672, 2006.

25   Dick, J., Skiba, U. and Wilson, J.: The Effect of Rainfall on NO and N2O Emissions from Ugandan Agroforest Soils, Phyton, 41, 73–80, 2001.

Dijkstra, F. A., Augustine, D. J., Brewer, P. and Fischer, von, J. C.: Nitrogen cycling and water pulses in semiarid grasslands: are microbial and plant processes temporally asynchronous? Oecol., 170, 799–808, doi:10.1007/s10021-010-9341-6, 2012.

30   Dorigo, W. A., Gruber, A., De Jeu, R. A. M., Wagner, W., Stacke, T., Loew, A., Albergel, C., Brocca, L., Chung, D., Parinussa, R. M. and Kidd, R.: Evaluation of the ESA CCI soil moisture product using ground-based observations, Remote Sens. Environ., 162, 380-395, doi:10.1016/j.rse.2014.07.023, 2014.

24

Dorigo, W., Wagner, W., Albergel, C., Albrecht, F., Balsamo, G., Brocca, L., Chung, D., Ertl, M., Forkel, M., Gruber, A., Haas, E., Hamer, P. D., Hirschi, M., Ikonen, J., de Jeu, R., Kidd, R., Lahoz, W., Liu, Y. Y., Miralles, D., Mistelbauer, T., Nicolai-Shaw, N., Parinussa, R., Pratola, C., Reimer, C., van der Schalie, R., Seneviratne, S. I., Smolander, T. and Lecomte, P.: ESA CCI Soil Moisture for improved Earth system understanding: State-of-the art and future directions, Remote Sens. Environ., 203, 185–215, doi:10.1016/j.rse.2017.07.001, 2017.

Duncan, B. N.: Interannual and seasonal variability of biomass burning emissions constrained by satellite observations, J. Geophys. Res.-Biol., 108, 73–28, doi:10.1029/2002JD002378, 2003.

Eickenscheidt, N., Brumme, R. and Veldkamp, E.: Direct contribution of nitrogen deposition to nitrous oxide emissions in a temperate beech and spruce forest – a ^{15}N tracer study, Biogeosci., 8, 621–635, doi:10.5194/bg-8-621-2011, 2011.

Emmerich, W. E.: Carbon dioxide fluxes in a semiarid environment with high carbonate soils, Agr. Forest Meteorol., 116, 91–102, doi:10.1016/S0168-1923(02)00231-9, 2003.

European Commission, Joint Research Center (JRC)/Netherlands Environmental Agency (PBL): Emission Database for Global Atmospheric Research (EDGAR), release version 4.2, [online] Available from: http://edgar.jrc.ed.europa.eu, 2011.

FAO: FAOSTAT database collections, [online] Available from: http://faostat.fao.org, Accessed January 2018

Galy-Lacaux, C. and Delon, C.: Nitrogen emission and deposition budget in West and Central Africa, Environ. Res. Lett., 9, 125002–14, doi:10.1088/1748-9326/9/12/125002, 2014.

Giglio, L., Randerson, J. T. and van der Werf, G. R.: Analysis of daily, monthly, and annual burned area using the fourth-generation global fire emissions database (GFED4), J. Geophys. Res.-Biogeosci., 118, 317–328, doi:10.1002/jgrg.20042, 2013.

Giglio, L., van der Werf, G. R., Randerson, J. T., Collatz, G. J. and Kasibhatla, P.: Global estimation of burned area using MODIS active fire observations, Atmos. Chem. Phys., 6, 957–974, doi:10.5194/acpd-5-11091-2005, 2006.

Gruber, A., Dorigo, W. A., Crow, W. and Wagner, W.: Triple Collocation-Based Merging of Satellite Soil Moisture Retrievals, IEEE Trans. Geosci. Remote Sens., 55, 6780–6792, doi:10.1109/TGRS.2017.2734070, 2017.

Hickman, J. E., Huang, Y., Wu, S., Diru, W., Groffman, P. M., Tully, K. L. and Palm, C. A.: Nonlinear response of nitric oxide fluxes to fertilizer inputs and the impacts of agricultural intensification on tropospheric ozone pollution in Kenya, Glob. Change Biol., 23, 3193-3204, doi:10.1029/95JD00370, 2017.

25

Holland, E., Braswell, B., Sulzman, J. and Lamarque, J.: Nitrogen deposition onto the United States and western Europe: Synthesis of observations and models, Ecol. Appl., 15, 38–57, 2005.

Huffman, G. J., Bolvin, D. T., Nelkin, E. J., Wolff, D. B., Adler, R. F., Gu, G., Hong, Y., Bowman, K. P. and Stocker, E. F.: The TRMM Multi-satellite Precipitation Analysis: Quasi-Global, Multi-Year, Combined-Sensor Precipitation Estimates at Fine Scale, J. Hydrometeorol., 8, 38–55, doi:10.1175/jhm560.1, 2007.

Huxman, T. E., Snyder, K. A., Tissue, D., Leffler, A. J., Ogle, K., Pockman, W. T., Sandquist, D. R., Potts, D. L. and Schwinning, S.: Precipitation pulses and carbon fluxes in semiarid and arid ecosystems, Oecol., 141, 254–268, doi:10.1007/s00442-004-1682-4, 2004.

Jacob, D. J.: Introduction to Atmospheric Chemistry, Princeton University Press, Princeton. 1999.

Jaeglé, L., Martin, R. V., Chance, K., Steinberger, L., Kurosu, T. P., Jacob, D. J., Modi, A. I., Yoboue, V., Sigha-Nkamdjou, L. and Galy-Lacaux, C.: Satellite mapping of rain-induced nitric oxide emissions from soils, J. Geophys. Res.-Biogeosci., 109, D21310, 2004.

Jena, C., Ghude, S. D., Blond, N., Beig, G., Chate, D. M., Fadnavis, S. and Van der A, R. J.: Estimation of the lifetime of nitrogen oxides over India using SCIAMACHY observations, Intl. J. Remote Sens., 35, 1244–1252, doi:10.1080/01431161.2013.873146, 2014.

Kieft, T., Soroker, E. and Firestone, M. K.: Microbial biomass response to a rapid increase in water potential when dry soil is wetted, Soil Biol. Biochem., 2, 119–126, 1987.

Kim, D. G., Vargas, R., Bond-Lamberty, B. and Turetsky, M. R.: Effects of soil rewetting and thawing on soil gas fluxes: a review of current literature and suggestions for future research, Biogeosci., 9, 2459–2483, doi:10.5194/bg-9-2459-2012, 2012.

Krotkov, N. A.: OMI/Aura NO2 Cloud-Screened Total and Tropospheric Column L3 Global Gridded 0.25 degree x 0.25 degree V3, doi:10.5067/Aura/OMI/DATA3007, Accessed January 2018.

Krotkov, N. A., Lamsal, L. N., Celarier, E. A., Swartz, W. H., Marchenko, S. V., Bucsela, E. J., Chan, K. L., Wenig, M. and Zara, M.: The version 3 OMI NO_2; standard product, Atmos. Meas. Tech., 10, 3133–3149, doi:10.5194/amt-10-3133-2017, 2017.

Lamarque, J. F., Bond, T. C., Eyring, V., Granier, C., Heil, A., Klimont, Z., Lee, D., Liousse, C., Mieville, A., Owen, B., Schultz, M. G., Shindell, D., Smith, S. J., Stehfest, E., Van Aardenne, J., Cooper, O. R., Kainuma, M., Mahowald, N., McConnell, J. R., Naik, V., Riahi, K. and van Vuuren, D. P.: Historical (1850–2000) gridded anthropogenic and biomass burning emissions of reactive gases and aerosols: methodology and application, Atmos. Chem. Phys., 10, 7017–7039, doi:10.5194/acp-10-7017-2010, 2010.

26

Lamsal, L. N., Krotkov, N. A., Celarier, E. A., Swartz, W. H., Pickering, K. E., Bucsela, E. J., Gleason, J. F., Martin, R. V., Philip, S., Irie, H., Cede, A., Herman, J., Weinheimer, A., Szykman, J. J. and Knepp, T. N.: Evaluation of OMI operational standard NO_2 column retrievals using in situ and surface-based NO_2 observations, Atmos. Chem. Phys., 14, 11587–11609, doi:10.5194/acp-14-11587-2014, 2014.

Laouali, D., Galy-Lacaux, C., Diop, B., Delon, C., Orange, D., Lacaux, J. P., Akpo, A., Lavenu, F., Gardrat, E. and Castera, P.: Long term monitoring of the chemical composition of precipitation and wet deposition fluxes over three Sahelian savannas, Atmos. Environ., 50, 314–327, doi:10.1016/j.atmosenv.2011.12.004, 2012.

Lelieveld, J., Evans, J. S., Fnais, M., Giannadaki, D. and Pozzer, A.: The contribution of outdoor air pollution sources to premature mortality on a global scale, Nature, 525, 367–371, doi:10.1038/nature15371, 2015.

Liu, Y. Y., Dorigo, W. A., Parinussa, R. M., de Jeu, R. A. M., Wagner, W., McCabe, M. F., Evans, J. P. and van Dijk, A. I. J. M.: Trend-preserving blending of passive and active microwave soil moisture retrievals, Remote Sens. Environ., 123, 280–297, doi:10.1016/j.rse.2012.03.014, 2012.

Masso, C., Nziguheba, G., Mutegi, J., Galy-Lacaux, C., Wendt, J., Butterbach-Bahl, K., Wairegi, L. and Datta, A.: Soil fertility management in sub-Saharan Africa, in Sustainable Agriculture Reviews, edited by E. Lichtfouse, Springer International Publishing, Cham. 2017.

McCalley, C. K. and Sparks, J. P.: Controls over nitric oxide and ammonia emissions from Mojave Desert soils, Oecol., 156, 871–881, doi:10.1007/s00442-008-1031-0, 2008.

McLinden, C. A., Fioletov, V., Boersma, K. F., Kharol, S. K., Krotkov, N., Lamsal, L., Makar, P. A., Martin, R. V., Veefkind, J. P. and Yang, K.: Improved satellite retrievals of NO_2 and SO_2 over the Canadian oil sands and comparisons with surface measurements, Atmos. Chem. Phys., 14, 3637–3656, doi:10.5194/acp-14-3637-2014, 2014.

McNally, A., Shukla, S., Arsenault, K. R., Wang, S., Peters-Lidard, C. D. and Verdin, J. P.: Int. J. Appl. Earth Obs., 48, 96–109, doi:10.1016/j.jag.2016.01.001, 2016.

Meixner, F. X., Fickinger, T., Marufu, L., Serca, D., Nathaus, F. J., Makina, E., Mukurumbira, L. and Andreae, M. O.: Preliminary results on nitric oxide emission from a southern African savanna ecosystem, Nutr. Cy. Agroecosys., 48., 123–138, 1997.

Nelson, D. W.: Gaseous Losses of Nitrogen Other Than Through Denitrification, in Nitrogen in Agricultural Soils, edited by F. J. Stevenson, pp. 327–363, dl.sciencesocieties.org, Madison. 1982.

Nicholson, S. E., Some, B., McCollum, J., Nelkin, E., Klotter, D., Berte, Y., Diallo, B. M., Gaye, I., Kpabeba, G., Ndiaye, O., Noukpozounkou, J. N., Tanu, M. M., Thiam, A., Toure, A. A. and Traore, A.

27

K.: Validation of TRMM and Other Rainfall Estimates with a High-Density Gauge Dataset for West Africa. Part I: Validation of GPCC Rainfall Product and Pre-TRMM Satellite and Blended Products, J. Appl. Meteorol., 42, 1337–1354, doi:10.1175/1520-0450(2003)042<1337:votaor>2.0.co;2, 2003.

Paulot, F. and Jacob, D. J.: Hidden Cost of U.S. Agricultural Exports: Particulate Matter from Ammonia Emissions, Environ. Sci. Technol., 48, 903–908, doi:10.1021/es4034793, 2014.

Pilegaard, K., Skiba, U., Ambus, P., Beier, C., Brüggemann, N., Butterbach-Bahl, K., Dick, J., Dorsey, J., Duyzer, J. and Gallagher, M.: Factors controlling regional differences in forest soil emission of nitrogen oxides (NO and N_2O), Biogeosci., 3, 651–661, 2006.

Placella, S. A. and Firestone, M. K.: Transcriptional Response of Nitrifying Communities to Wetting of Dry Soil, Appl. Environ. Microbiol., 79, 3294–3302, doi:10.1128/AEM.00404-13, 2013.

Placella, S. A., Brodie, E. L. and Firestone, M. K.: Rainfall-induced carbon dioxide pulses result from sequential resuscitation of phylogenetically clustered microbial groups, Proc. Nat. Acad. Sci., 109, 10931–10936, 2012.

Potter, C. S., Randerson, J. T., Field, C. B., Matson, P. A., Vitousek, P. M., Mooney, H. A. and Klooster, S. A.: Terrestrial ecosystem production: A process model based on global satellite and surface data, Glob. Biogeochem. Cy., 7, 811–841, doi:10.1029/93GB02725, 1993.

Praveen-Kumar and Aggarwal, R. K.: Interdependence of ammonia volatilization and nitrification in arid soils, Nutr. Cy. Agroecosys., 51, 201–207, doi:10.1023/A:1009720003490, 1998.

Randerson, J. T., Chen, Y., van der Werf, G. R., Rogers, B. M. and Morton, D. C.: Global burned area and biomass burning emissions from small fires, J. Geophys. Res.—Biogeosci., 117, G04012, doi:10.1029/2012JG002128, 2012.

Robertson, G. P. and Groffman, P. M.: Nitrogen transformations, edited by E. A. Paul, pp. 341–364, Soil microbiology, ecology, and biochemistry, 3rd edn. Academic/Elsevier, New York. 2007.

Robinson, T. P., Wint, G. R. W., Conchedda, G., Van Boeckel, T. P., Ercoli, V., Palamara, E., Cinardi, G., D'Aietti, L., Hay, S. I. and Gilbert, M.: Mapping the Global Distribution of Livestock, PLoS ONE, 9, e96084, doi:10.1371/journal.pone.0096084, 2014.

S Whitburn, S., . van Damme, M., Clarisse, L., Bauduin, S., Heald, C. L., Hadji-Lazaro, J., Hurtmans, D., Zondio, M.A., Clerbaux, C., Coheur, P.-F.: A flexible and robust neural network IASI-NH3 retrieval algorithm, J. Geophys. Res.—Biogeosci., 121, 6581-6599, doi:10.1002/(ISSN)2169-8996, 2016.

Saetre, P. and Stark, J. M.: Microbial dynamics and carbon and nitrogen cycling following re-wetting of soils beneath two semi-arid plant species, Oecol., 142, 247–260, doi:10.1007/s00442-004-1718-9, 2004.

28

Schlesinger, W. H. and Peterjohn, W. T.: Processes controlling ammonia volatilization from Chihuahuan desert soils, Soil Biol. Biochem., 23, 637–642, 1991.

Semb, G. and Robinson, J. B. D.: The natural nitrogen flush in different arable soils and climates in East Africa, E. Afr. Agric. Forestry J., 34, 350–370, 1969.

5 Sheahan, M. and Barrett, C. B.: Ten striking facts about agricultural input use in Sub-Saharan Africa, Food Policy, 67, 12–25, doi:10.1016/j.foodpol.2016.09.010, 2017.

Slessarev, E. W., Lin, Y., Bingham, N. L., Johnson, J. E., Dai, Y., Schimel, J. P. and Chadwick, O. A.: Water balance creates a threshold in soil pH at the global scale, Nature, 540, 567–569, doi:10.1038/nature20139, 2016.

10 Soper, F. M., Boutton, T. W., Groffman, P. M. and Sparks, J. P.: Nitrogen trace gas fluxes from a semiarid subtropical savanna under woody legume encroachment, Glob. Biogeochem. Cy., 30, 614–628, doi:10.1002/2015gb005298, 2016.

Thomas, R. Q., Canham, C. D., Weathers, K. C. and Goodale, C. L.: Increased tree carbon storage in response to nitrogen deposition in the US, Nature Geosci., 3, 13–17, doi:10.1038/ngeo721, 2009.

15 Tian, D. and Niu, S.: A global analysis of soil acidification caused by nitrogen addition, Environ. Res. Lett., 10, 024019–11, doi:10.1088/1748-9326/10/2/024019, 2015.

Van Damme, M., Clarisse, L., Heald, C. L., Hurtmans, D., Ngadi, Y., Clerbaux, C., Dolman, A. J., Erisman, J. W. and Coheur, P. F.: Global distributions, time series and error characterization of atmospheric ammonia, Atmos. Chem. Phys., 14, 2905–2922, doi:10.5194/acp-14-2905-2014, 2014.

20 Van Damme, M., Erisman, J. W. and Clarisse, L.: Worldwide spatiotemporal atmospheric ammonia (NH3) columns variability revealed by satellite, Geophys. Res. Lett., 42, 8660–8668, doi:10.1002/(ISSN)1944-8007, 2015.

van der Werf, G. R., Randerson, J. T., Giglio, L., van Leeuwen, T. T., Chen, Y., Rogers, B. M., Mu, M., van Marle, M. J. E., Morton, D. C., Collatz, G. J., Yokelson, R. J. and Kasibhatla, P. S.: Global fire
25 emissions estimates during 1997–2016, Earth Syst. Sci. Data, 9, 697–720, doi:10.5194/essd-9-697-2017, 2017.

Vågen, T.-G., Winowiecki, L. A., Tondoh, J. E., Desta, L. T. and Gumbricht, T.: Mapping of soil properties and land degradation risk in Africa using MODIS reflectance, Geoderma, 263, 216–225, doi:10.1016/j.geoderma.2015.06.023, 2016.

30 Vrieling, A., de Beurs, K. M. and Brown, M. E.: Variability of African farming systems from phenological analysis of NDVI time series, Clim. Change, 109, 455–477, doi:10.1029/2004JD005263, 2011.

Whitburn, S., Van Damme, M. and Clarisse, L.: A flexible and robust neural network IASI-NH3 retrieval algorithm, J. Geophys. Res.-Atmos., 121, 6581–6599, doi:10.1002/(ISSN)2169-8996, 2016.

Whitburn, S., Van Damme, M., Kaiser, J. W., van der Werf, G. R., Turquety, S., Hurtmans, D., Clarisse, L., Clerbaux, C. and Coheur, P. F.: Ammonia emissions in tropical biomass burning regions: 5 Comparison between satellite-derived emissions and bottom-up fire inventories, Atmos. Environ., 121, 42–54, doi:10.1016/j.atmosenv.2015.03.015, 2015.

Yahdjian, L. and Sala, O. E.: Size of Precipitation Pulses Controls Nitrogen Transformation and Losses in an Arid Patagonian Ecosystem, Ecosystems, 13, 575–585, doi:10.1007/s10021-010-9341-6, 2010.

10 Yang, Y., Zhou, C., Li, N., Han, K., Meng, Y., Tian, X. and Wang, L.: Effects of conservation tillage practices on ammonia emissions from Loess Plateau rain-fed winter wheat fields, Atmos. Environ., 104, 59–68, doi:10.1016/j.atmosenv.2015.01.007, 2015.
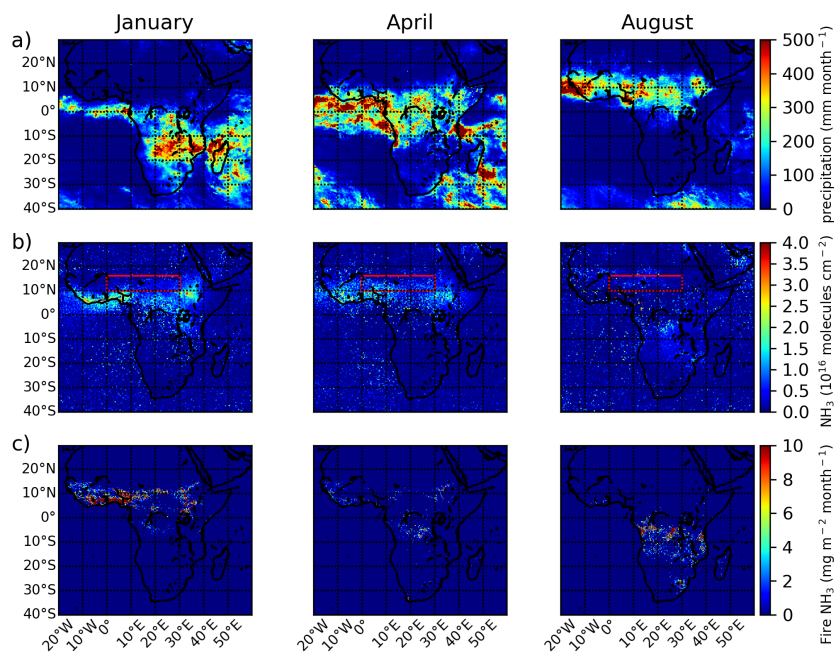
Figure 1. *Seasonality of precipitation and NH₃ emissions in Africa during 2008.* Monthly TRMM precipitation (a), IASI-NH₃ concentrations (b), and GFED4s NH₃ emissions (c) over Africa in January, April, and August, 2008. TRMM precipitation is presented in mm month^{-1}, IASI-NH₃ concentrations in 10^{16} molecules cm^{-2}, and GFED4s NH₃ emissions in mg m^{-2} month^{-1}.

Commented [Gv1]: Please adjust ylabel in figure
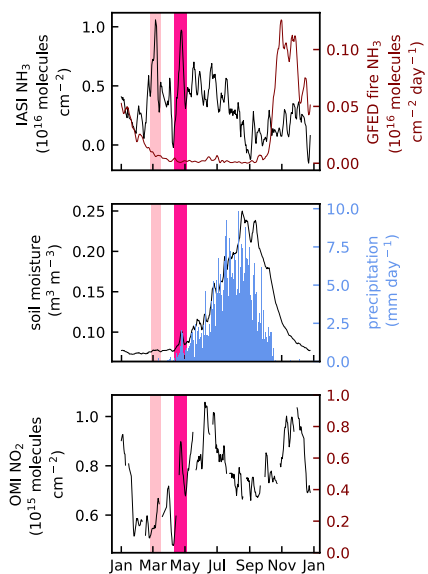
Figure 2: *Early growing season NH₃ pulses temporally associated with changes in soil moisture and with NO₂ pulses over the focal study region in the Sahel during 2008*. Top panel: Daily atmospheric NH₃ concentrations from IASI and NH₃ biomass burning emissions from GFED4s. Middle panel: ESA-CCI soil moisture and TRMM precipitation. Bottom panel: atmospheric NO₂ concentrations from OMI. Putative soil emission pulses in March and April are highlighted in bright and dark pink, respectively. Mean NO₂ concentrations were calculated using values of 0.25° grid cells within the study region for which NH₃ observations were also present. GFED4s emissions were converted from a mass-based to molecule-based flux to allow comparison with the IASI retrievals; note the different scales for the left and right y axes of the top panel.
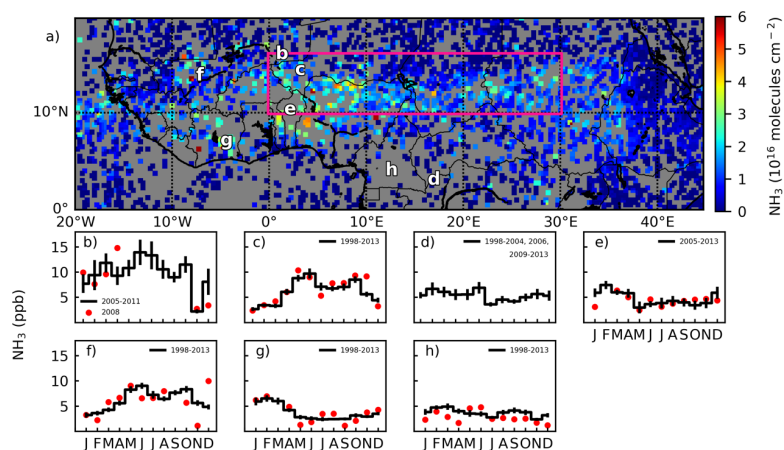
Figure 3. *NH₃ pulsing over the Sahel in April, and geographic variation in the seasonality of surface NH₃ concentrations over north equatorial Africa.* (a) Observations by IASI during April 25 to April 28, 2008 reveal elevated mean atmospheric NH₃ concentrations specifically over the Sahel region (b-h). Monthly NH₃ gas concentrations from sites in the INDAAF network; black lines represent the multi-year mean and standard error for each site, and red dots represent the 2008 value. Data are presented for Agoufou, Mali (b), Banizoumbou, Niger (c), Bomassa, Congo (d), Djougou, Benin (e), Katibougou, Mali (f), Lamto, Côte d'Ivoire (g), and Zoetele, Cameroon (h).
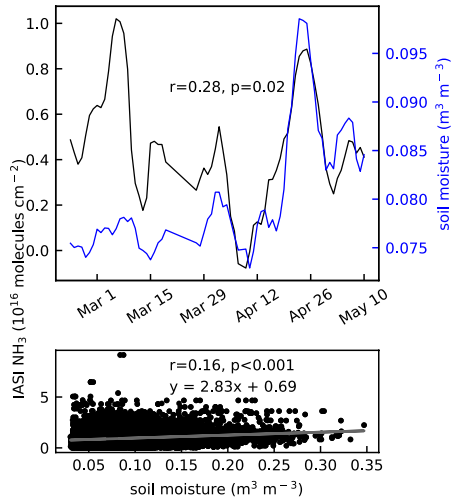
Figure 4. *Correlations between soil moisture and atmospheric NH3 concentrations observed by IASI over the focal study region in the Sahel during the start of the rainy season in 2008.* Top panel: 5-day running mean of daily NH3 concentrations and daily soil moisture for the focal study region from mid-February through the end of April, 2008. Bottom panel: scatterplot of soil moisture versus atmospheric NH3 concentration for each 0.25° grid cell in the study region during April, 2008. In both panels, soil moisture data are included only for those 0.25° grid cells where NH3 observations are available for the same day.

Deleted: pixel
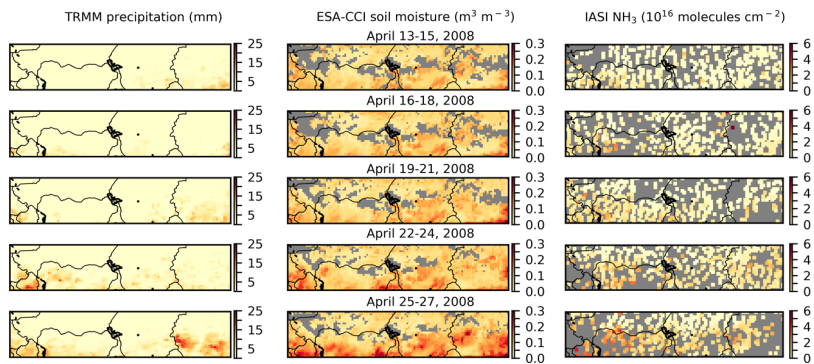
Figure 5. Maps of changing precipitation, soil moisture, and atmospheric NH$_3$ concentrations for the focal region of the Sahel during the second half of April, 2008. 3-day averages from April 13 through April 27 are presented for precipitation from TRMM (left column), soil moisture from ESA-CCI (middle column) and atmospheric NH$_3$ concentrations for acceptable retrievals from IASI (right column).
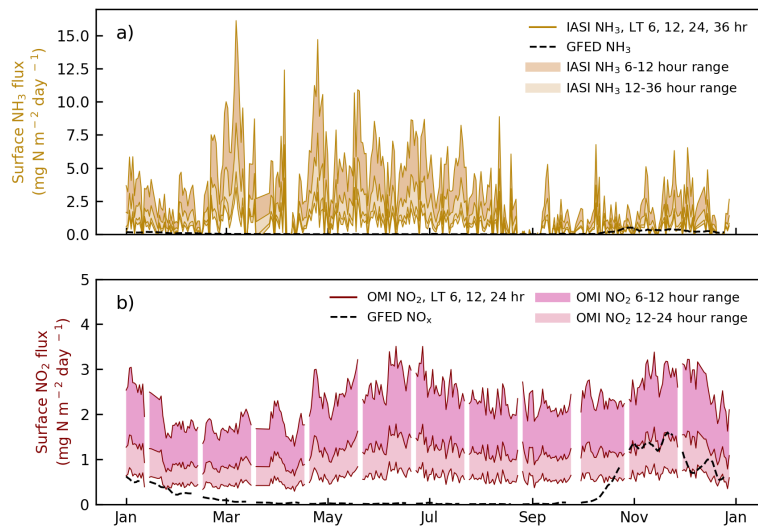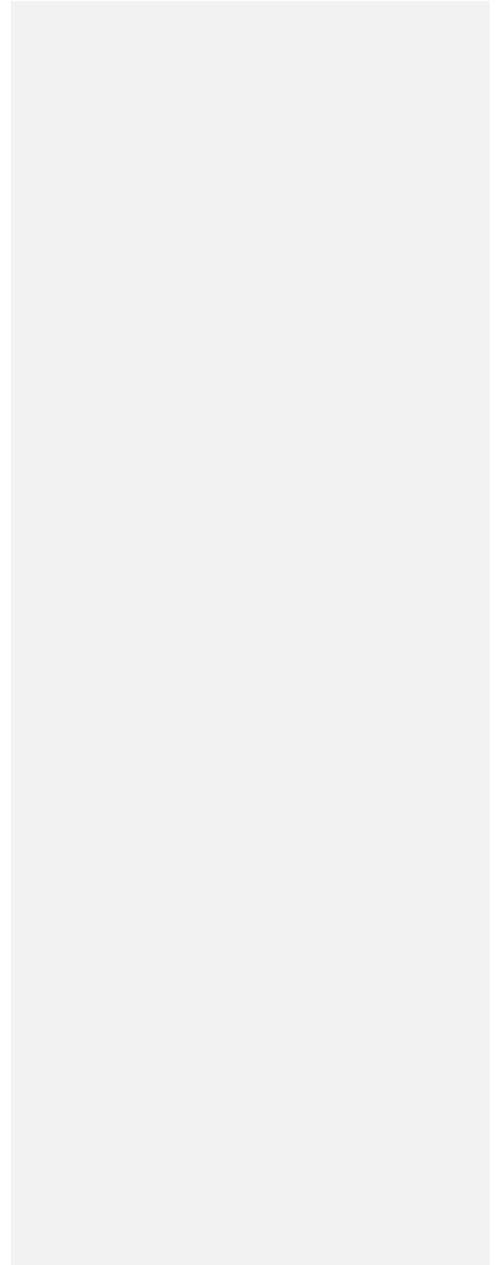
Figure 6. *Comparison of daily total surface fluxes and biomass burning emissions of a) NH₃-N and b) NO₂-N for the focal study region in the Sahel during 2008.* Total surface fluxes are estimated from IASI NH₃ and OMI NO₂ observations using a simple box model and assuming effective lifetimes of 12, 24, or 36 hours for NH₃ and of 6, 12, or 24 hours for NO₂. Fire emissions are taken from the GFED4s database. Modelled NO₂ emissions were calculated using values of 0.25° grid cells within the study region for which NH₃ observations were also present. GFED4s emission means were calculated using 0.25° grid cells that matched those used in the modelled emissions for the respective gas. Note the difference in scales, and that shorter effective lifetimes result in higher modelled emissions.
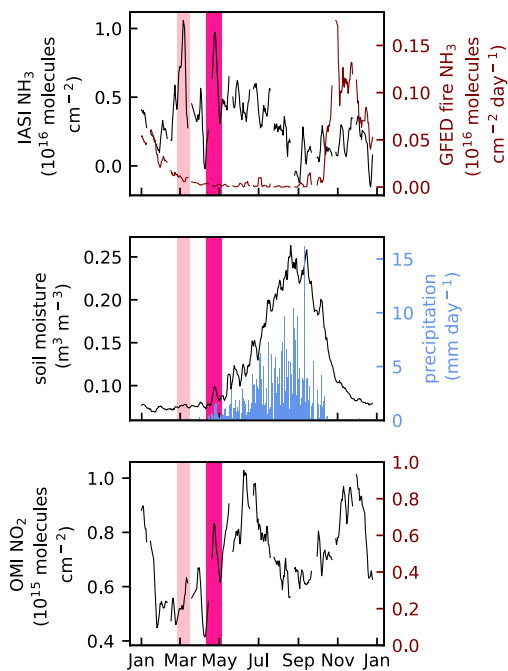
Figure S1: *Early growing season NH₃ pulses temporally associated with changes in soil moisture and with NO₂ pulses over the focal study region in the Sahel during 2008.* Top panel: Daily atmospheric NH₃ concentrations from IASI and NH₃ biomass burning emissions from GFED4s. Middle panel: ESA-CCI soil moisture and TRMM precipitation. Bottom panel: atmospheric NO₂ concentrations from OMI. Putative soil emission pulses in March and April are highlighted in bright and dark pink, respectively. The means of all variables presented were calculated using values of 0.25° grid cells within the study region for which both NO₂ and NH₃ observations were present. GFED4s emissions were converted from a mass-based to molecule-based flux to allow comparison with the IASI retrievals; note the different scales for the left and right y axes of the top panel.
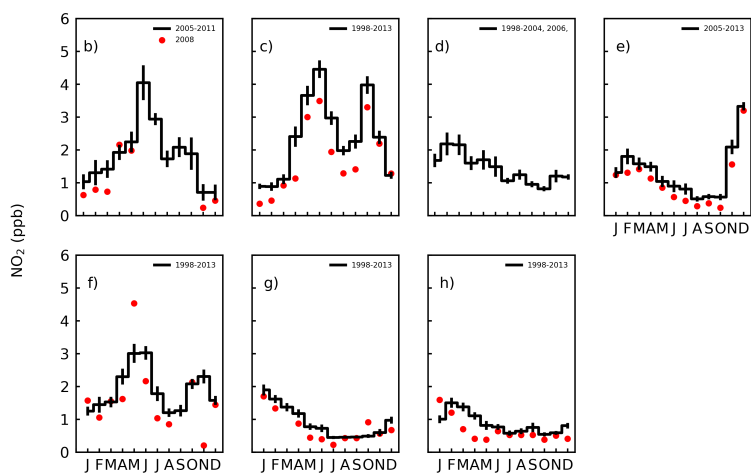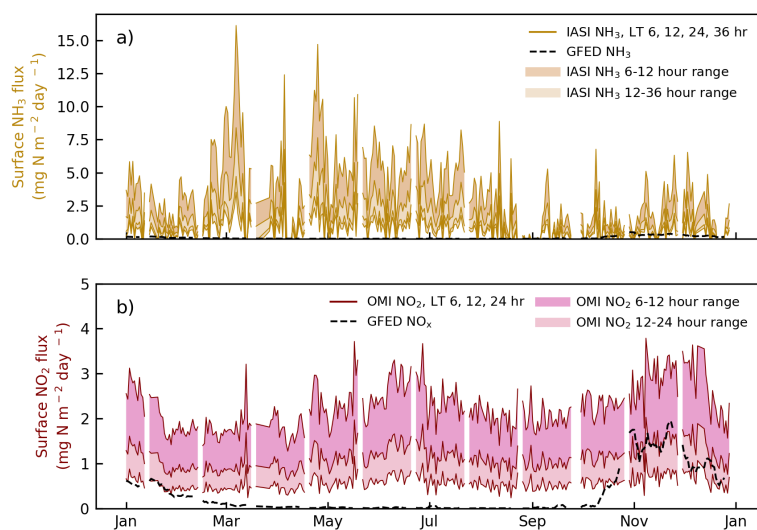
Figure S2. *Geographic variation in the seasonality of surface NO$_2$ concentrations over north equatorial Africa.* Monthly NO$_2$ gas concentrations from sites in the INDAAF network; black lines represent the multi-year mean and standard error for each site, and red dots represent the 2008 value. Data are presented for Agoufou, Mali (b), Banizoumbou, Niger (c), Bomassa, Congo (d), Djougou, Benin (e), Katibougou, Mali (f), Lamto, Côte d'Ivoire (g), and Zoetele, Cameroon (h). Note that there is no panel (a) in this figure, so that the site labels match those in Figure 3.

Figure S3. *Comparison of daily total surface fluxes and biomass burning emissions of a) NH₃-N and b)*
NO₂-N for the focal study region in the Sahel during 2008. Total surface fluxes are estimated from IASI
NH_3 and OMI NO_2 observations using a simple box model and assuming effective lifetimes of 12, 24, or
36 hours for NH_3 and of 6, 12, or 24 hours for NO_2. Fire emissions are taken from the GFED4s database.
Modelled and GFED4s mean emissions were calculated using values only of 0.25° grid cells within the
study region for which both NO_2 and NH_3 observations were present. Note the difference in scales, and
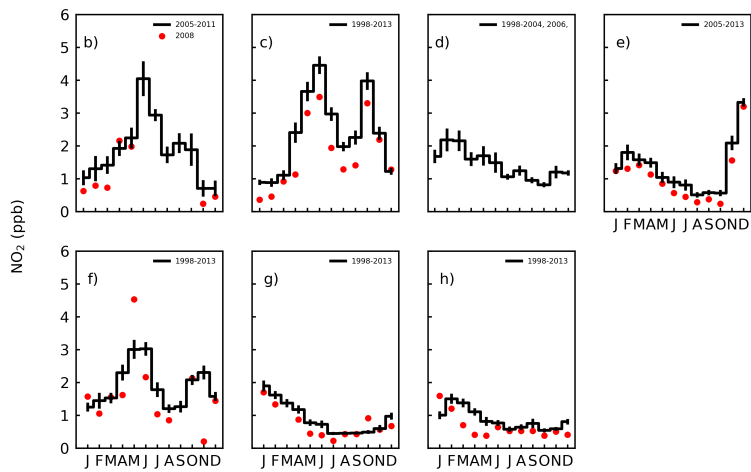that shorter effective lifetimes result in higher modelled emissions.

Figure S4. *Monthly means of IASI observations of atmospheric NH₃ concentrations for 1° grid cells centered over Agoufou, Mali, Banizoumbou, Niger and Katibougou, Mali in 2008.* Surface observations for each site are presented in Figure 3b, 3c, and 3f, respectively.

5